DELAYED COINCIDENCE SPECTROSCOPY OF FISSION FRAGMENT EXCITED GASES

By

GEORGE ROBERT SHIPMAN

A DISSERTATION PRESENTED TO THE GRADUATE COUNCIL OF
THE UNIVERSITY OF FLORIDA
IN PARTIAL FULFILLMENT OF THE REQUIREMENTS FOR THE
DEGREE OF DOCTOR OF PHILOSOPHY

UNIVERSITY OF FLORIDA

1976

ACKNOWLEDGMENTS

As with any research effort, this dissertation has not been the result of one person's efforts. The patient and fatherly concern of Professor R. T. Schneider in the continued support of this project is gratefully acknowledged. The willingness of my chairperson, H. D. Campbell, to provide help and insights into the theoretical aspects of fission fragment produced plasmas was balanced by the equal and complementary efforts of E. E. Carroll who suggested the path through two apparently insoluable experimental difficulties. Mr. Ken Fawcett, a man with an uncanny ability to revive aged and senile electronic equipment, provided for the care and well-being of the detection system. Mr. Ernie Whitman and Mr. Joe Mueller provided help and expertise in numerous and diverse fields. I have benefited from discussions with many of my fellow students but especially Drs. Bob Davie, John Davis and Jim Fuller. I have also had the benefit of four friends and helpers during the course of this research. Dave Sterritt and George Strickland devised and wrote the programs for the data reduction while Dudley Carter helped in almost every phase of the work. I pass this system and the remaining problems on to Tom Maguire who has been of immense help in the later stages of this work. I wish to thank my wife, Barbara Jo, for typing and

and retyping the rough draft and for her nearly patient encouragement during the long term of this effort.

TABLE OF CONTENTS

LIST OF FIGURES

Abstract of Dissertation Presented to the
Graduate Council of the University of Florida
in Partial Fulfillment of the Requirements for the
Degree of Doctor of Philosophy

DELAYED COINCIDENCE SPECTROSCOPY OF FISSION FRAGMENT EXCITED GASES

By

George Robert Shipman

December, 1976

Chairman: Hugh D. Campbell, Ph.D.
Major Department: Nuclear Engineering Sciences

A time resolved single photon counting system was used to study the emission spectra of N_2 under fission fragment bombardment. The source of fission fragments was 0.01μg of ^{252}Cf evaporated on a platinum disk. The ^{252}Cf emitted two groups of fission fragments with energies of about 80 MeV and about 105 MeV at a rate of 6,000 per second.

The system used a time-to-amplitude converter (TAC) which converted the time difference between two timing signals into a voltage. The "start" pulse was supplied by a plastic scintillator which detected the prompt fission gamma rays. The "stop" pulse was generated when a single photon struck the photomultiplier mounted on the spectrograph. The probability that a photon occurred was proportional to the population of the excited state giving rise to the observed spectral line. The number of photons in each time interval was thus related to the excited state density in that same time interval. After accumulating enough counts to give acceptable statistics, a curve

was generated which plotted the number density of excited states as a function of time-after-fission. The portion of the curve which occurred after the fission fragment had passed out of the field of view (the afterglow) was least squares fitted to a decreasing exponential.

It was observed that the excited state population decayed more rapidly as the pressure was increased. Extrapolation to zero pressure allowed determination of the radiative lifetime while the rate of change of decay time with pressure was related to the collisional quenching cross section. The resolving time of this system was less than two nanoseconds.

The radiative lifetime of $N_2(C^3\Pi u)$ was found to be 42ns±1.5ns and the collisional transfer rate constant to be $1.0 \times 10^{-11} cm^3 sec^{-1}$.

Several other noble gas-nitrogen mixtures are described in a more qualitative manner.

CHAPTER I

INTRODUCTION

1.1 Background

This dissertation is divided conceptually into three parts. First, there is the description of a new system which was developed for the analysis of gases excited by non-periodic, transient, randomly occurring events. Second, this system was used to make a careful study of one particular excited level in one particular gas. Third, a more qualitative description is given of some measurements which were done on various gas mixtures exhibiting both resonant and nonresonant behavior.

The work which led to this dissertation was initially conceived as an alternative to an in-core reactor experiment. The study of fission fragment excited gases had been going on for some time in connection with both the gaseous core reactor and the nuclear pumped laser program.[1,2,3,4] A typical experiment involved placing a ^{235}U lined cylinder within the core of the reactor, filling the cylinder with a chosen gas or gas mixture, and observing the emitted photons with a spectrographic system.[1,2] There were, however, several limitations inherent in this type of experiment. Because of the nature of the reactor environment, stringent safety precautions had to be maintained. These precautions, while

necessary, severely limited access to the experimental device and restricted data acquisition, system modification, and system adjustment. Excitation using the spontaneous fission fragment emitter ^{252}Cf was seen as an attractive alternative. This isotope provides a safe, small, self-powered source of energetic fission fragments closely resembling in all respects the fission fragments emitted by ^{235}U (see Appendix 6). At first it was thought that the extremely low flux, about nine orders of magnitude less than in the reactor, would make the spectroscopic diagnostics an insuperably difficult problem. The resolution of this problem proved to be the adoption of single photon counting techniques.

1.2 General Description

Preliminary intensity measurements indicated that only about one photon was observed for each 100 fission fragments which passed through the region of observation. In addition, it was soon realized that the time that a fission fragment took to cross the chamber (about four nanoseconds) and, hence, the length of the excitation pulse was extremely short as compared to the mean time between fission fragments (about 0.3 milliseconds) thus allowing a unique assignment of an observed photon to a particular fission fragment. Since we could tell which fission fragment caused which photon, a measurement of the time interval between the passage of the fission fragment and the emission of the photon allowed a determination of the lifetime of the atomic

or molecular level from which the photon originated. We had thus created a fluorescence decay system utilizing a totally new type of excitation. Since the probability that a photon will be observed at a certain point in time is proportional to the population density at that time, a history of the photon flux is a history of the excited state population. After the time intervals between many fission fragment-photon pairs had been measured, such a photon flux history was obtained. Determination of the interval between excitation and photon emission required accurate knowledge of when the fission fragment transited the excitation region. In all previous fluorescence decay systems, the excitation source had been triggerable, and this trigger had provided the timing "start" pulse. Here, however, the excitation was a randomly occurring, non-periodic, transient event. Two independent methods were developed for providing the timing "start" pulse, both of which were found to give identical results.

What originally started as an alternative to a reactor experiment evolved into a system of great versatility, capable of providing information not only about fission fragment excited gases, but also about the fluorescence decay of atomic and molecular levels.

The extent to which the information obtained in this experiment can be scaled to the reactor situation has not yet been resolved. Several studies[1 2 3] have shown that population density increases linearly with reactor power

over several orders of magnitude. Populations probably remain linear until electron-electron interactions begin to dominate the thermalization of the swarm, a density which has not yet been reached in gases up to one atmosphere.

1.3 Previous Work

Previous work germane to this dissertation has appeared in a diverse range of fields. This work has been recently reviewed[4] and the interested reader is referred thereto. If, from the vast body of literature available upon the subject of the interactions of fast charged particles with gases, we restrict our attention to those which are concerned with the passage of fission fragments and the subsequent emission of photons, we find that they are, with one exception, concerned with the steady state case of excitation within a reactor. That exception is the work of Axtmann[5] and his students at Princeton. They have also studied the $C^3\Pi u$ level of nitrogen, but with quite a different experimental technique and obtained essentially identical results.

1.4 Organizational Plan

The plan of this dissertation will be to first develop in Chapter 2 the theory necessary to understand the optical emission of fission fragment excited gases in a general way, and then look at the rate equations for the $C^3\Pi u$ level in pure nitrogen. In Chapter 3 will be described the experimental apparatus and its calibration. Chapter 4 will be an analysis of the results for pure nitrogen, including values

for the radiative and collisional rate constants. Chapter 5 will describe in a semiquantitative way the measurements which have been made on other gases and gas mixtures. After a short concluding discussion, a series of appendices will examine in greater detail some questions which relate to the analysis rather than interpretation of the results.

CHAPTER 2

THEORETICAL CONSIDERATIONS

2.1 Introduction

The primary theoretical motivation for this dissertation was the desire to understand in what respect plasmas created by the passage of fast charged particles resembled (and how they differed from) electrically produced plasmas. During the early stages of the research, which eventually led to a nuclear pumped laser, it was widely believed that plasmas created by ionizing radiation would differ in fundamental respects from electrical plasmas. As more insight was gained, however, it was realized that the bulk of the excitation and ionization was caused by the shower of fast secondary electrons rather than by the fission fragment itself.[6] Thus the excitation process was seen to be electron impact excitation with the following difference: the electron energy distribution was nonmaxwellian, with peaks at high energies corresponding to the "injection" energy of the secondary electrons.[7] Since, in the nuclear plasma case, the electrons are always slowing down from their initial birth energy, while, in an electrical plasma, the electrons are being constantly accelerated by the electric field, we may expect some differences in the excited state populations.

The basic operational problem was that of finding relations between the observable quantity N(t), the number of photons which were emitted at time "t" after fission, and the properties of fission fragment excited gases in general or atomic and molecular properties of particular gases. We shall first describe the interaction of the fission fragment with the gas in a general way, and then, these relations will be derived by starting with the elementary rate equations for pure nitrogen. The parameters most amenable to analysis were τ, the 1/e decay time; τ_{rise}, the 1/e rise time; ΣN_i, the sum of all photons observed independent of time; and N_{max}, the value of the peak intensity (see Fig. 1).

2.2 Fission Fragment — Gas Interactions

Californium was chosen as a fission fragment source since it underwent spontaneous fission and, thus, eliminated the need for a neutron supply as is the case with uranium. When a spontaneous fission occurred, the first particles which entered the gas were prompt gamma rays. These gammas were emitted within 10^{-11} seconds of fission, but caused little excitation of the gas in the experimental chamber. They could, however, cause a small ionization pulse in the residual gas within the photomultiplier. This pulse was amplified by the dynodes and recorded by the counting system. The gamma pulse occurred well before the peak of the light pulse, and caused no increase in background during the decay period. (see Fig. 2). At the time of

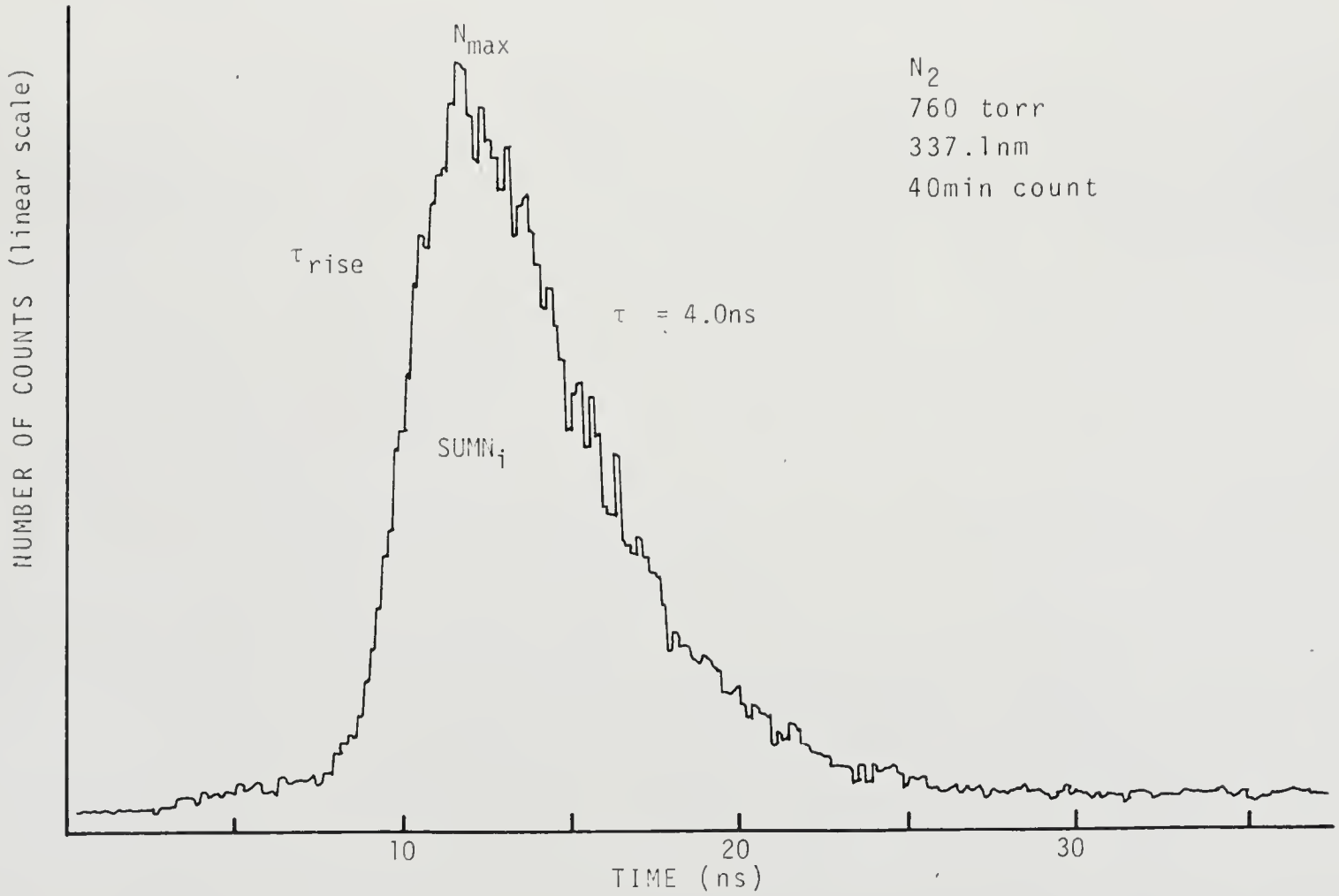

Figure 1. Typical I(t) Curve

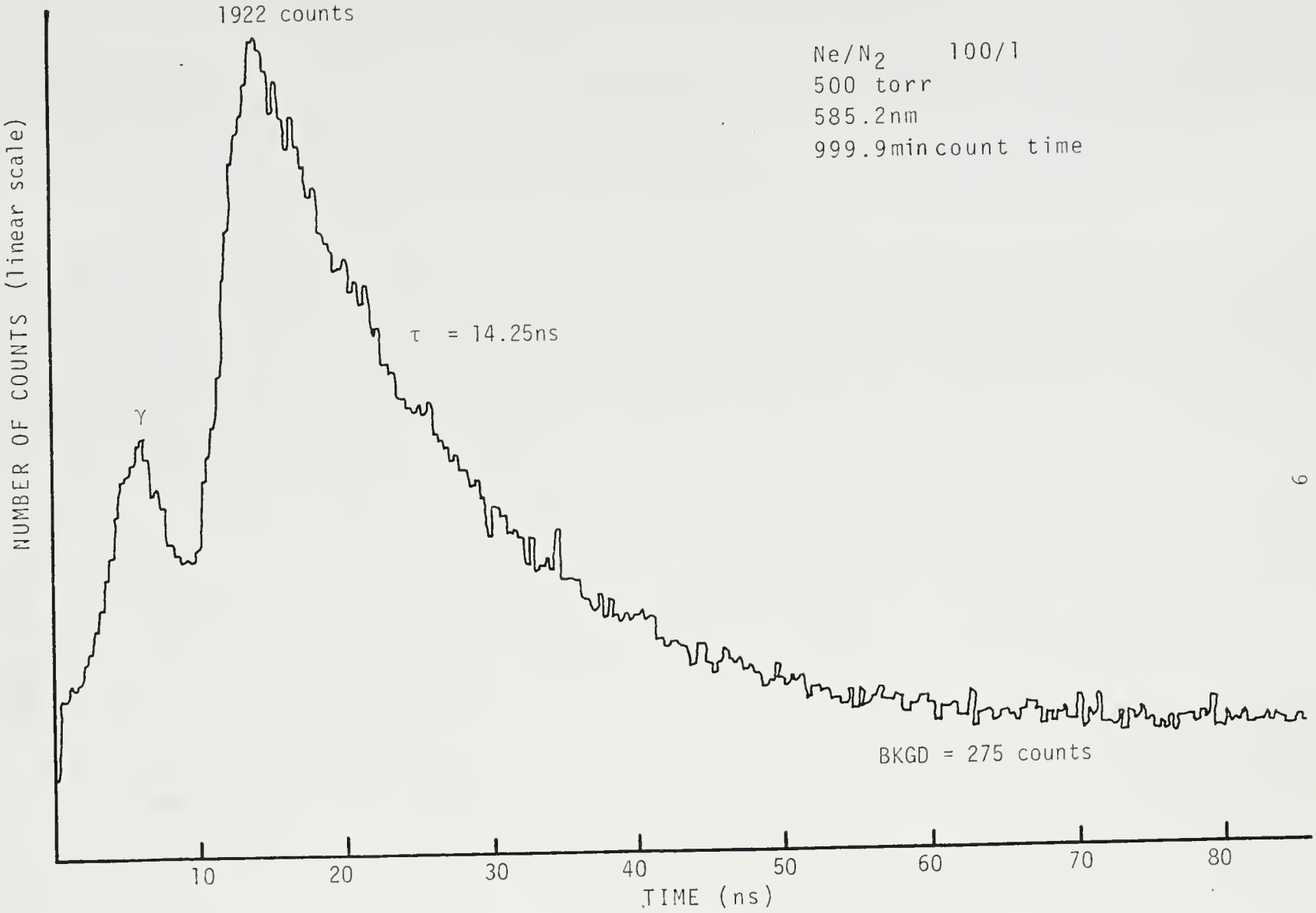

Figure 2. Typical Decay Curve Showing γ Coincidence Peak

the gamma burst, the fission fragments began to enter the gas. As the fission fragments passed through the gas, they struck atoms of the gas mixture causing excitation and ionization. The resulting excited states and ion pairs were not all produced in interactions with the fission fragment. The bulk of the excitation and ionization was produced by the secondary electrons ejected during the ionization.

Once the fission fragment had stopped, either by giving up its energy or through hitting the wall, no more energy was transferred to the gas, and relaxation proceeded (see Appendix 5). Though no more energy was entering the gas as a whole, the populations of individual levels may still have continued increasing. This continued increase may have been due to dissociative recombination, cascading, resonance trapping, or metastable transfer. In these cases it was difficult to say exactly when the excitation of a given level ended, and the afterglow commenced. Thus, while the decay rate in the afterglow was determined by the radiative and collisional lifetimes, if excitation processes continued after the fission fragment had passed from view, then what was being measured was the excitation or transfer rate rather than the decay rate.

We have now followed the energy of the fission fragment in a general way from the time the fragment entered the gas until some of its energy reached a particular atomic or molecular level. The energy thus stored in a

level may leave by a variety of routes. The energy pathways for deexcitation depend upon pressure in a complicated way, because collisional effects are a function of pressure. At very low pressures where collisions may be ignored, the major loss of energy from a level is due to radiative decay. As the pressure increases, collisional self-quenching will cause the lifetime of the level to decrease (see Figs. 3 and 4). By extrapolating the lifetime versus pressure curve back to zero pressure, the radiative lifetime may be determined. Fig. 5. Thus, the rate at which the lifetime changed with pressure may be used to determine the collisional transfer coefficient for the observed level. This discussion of deexcitation assumes that no impurities are present. With impurities, the kinetic behavior becomes a great deal more complicated. Impurity quenching may cause the lifetime of a level to decrease from what it was in the pure gas case, while the effects of transfer from an impurity with a resonant metastable level can cause a dramatic increase (see Fig. 6). If two different deexcitation paths exist having quite different time scales, the decay curve may show two decay times, one for short times and one for long times (see Fig. 7).

With the exception of a small amount of work on CF_4, the bulk of this study was carried out on the gases helium, neon, argon, and nitrogen. Partial energy level diagrams for these gases are shown in Figure 8. This figure illustrates the energetic resonance between the

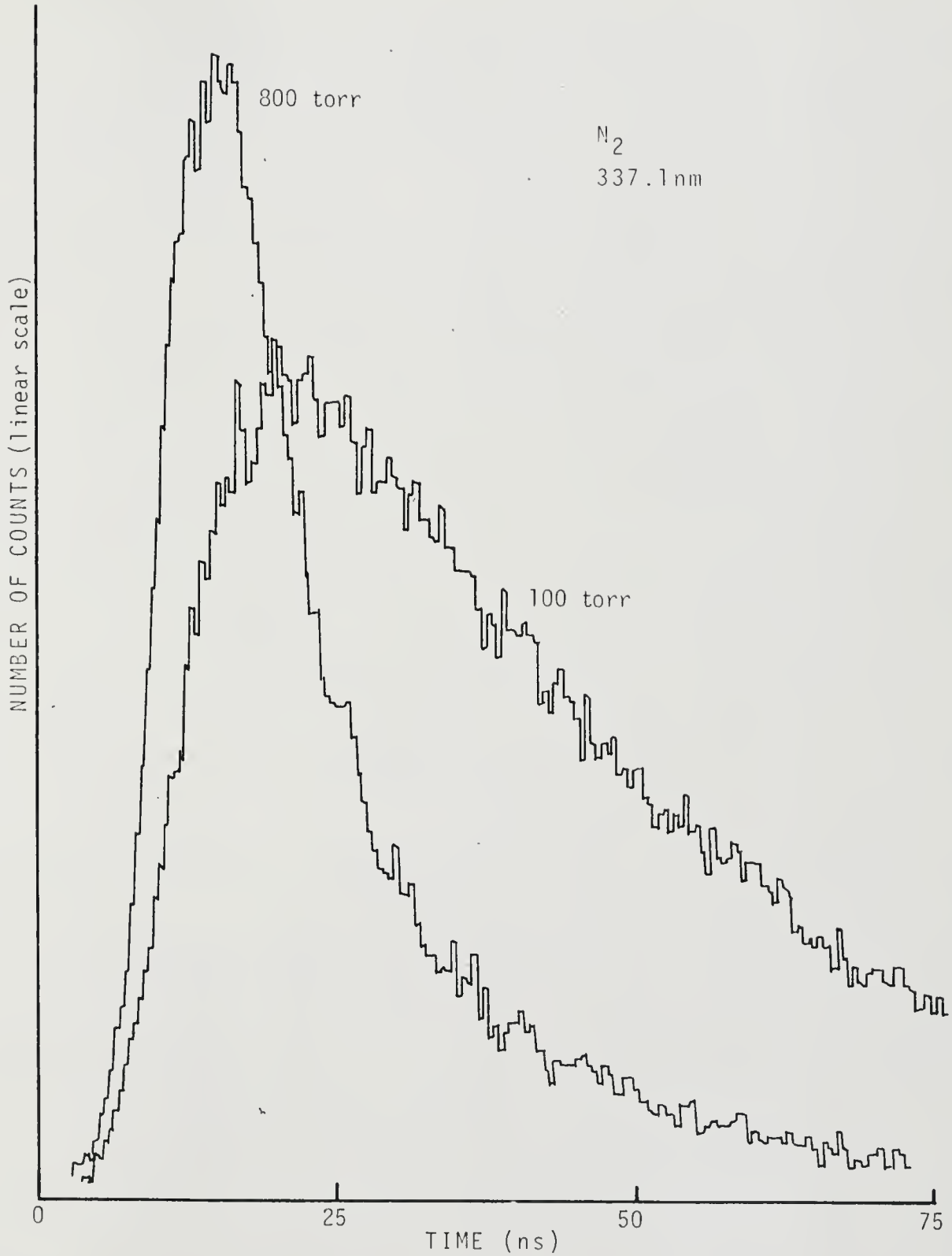

Figure 3. Pressure Variation of Decay Time

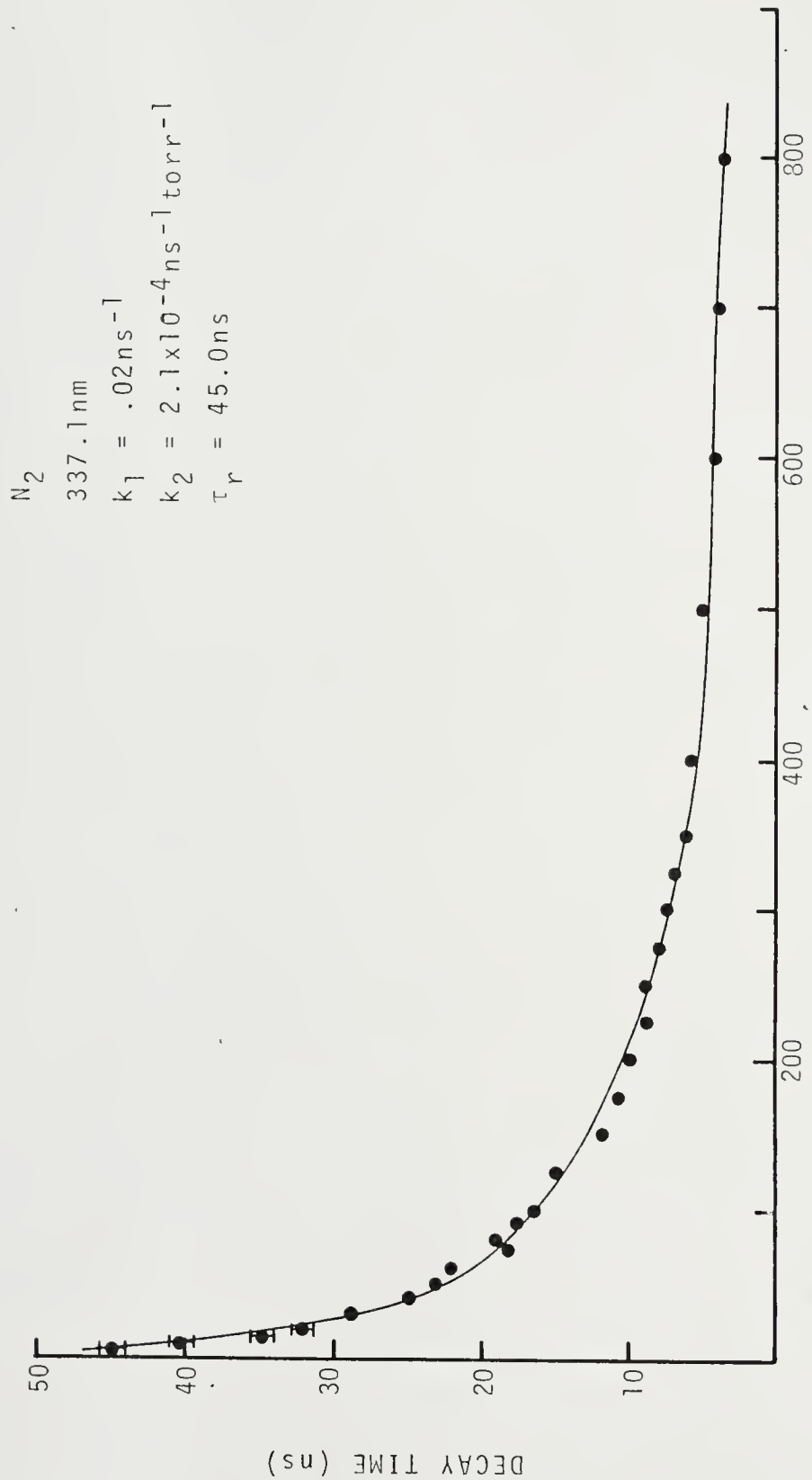

Figure 4. Decay Time Versus Pressure for 337.1nm

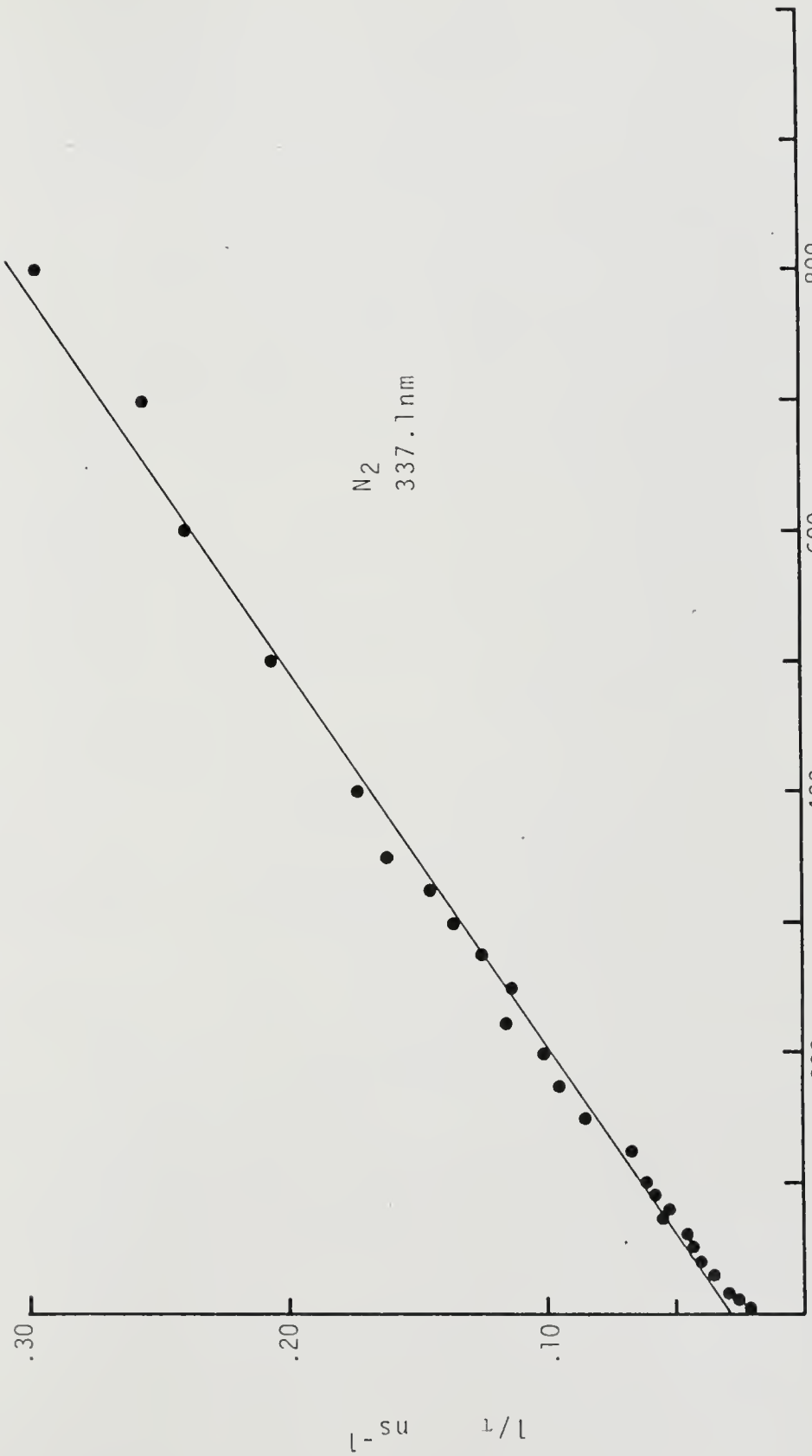

Figure 5. Inverse Decay Time Versus Pressure for 337.1nm

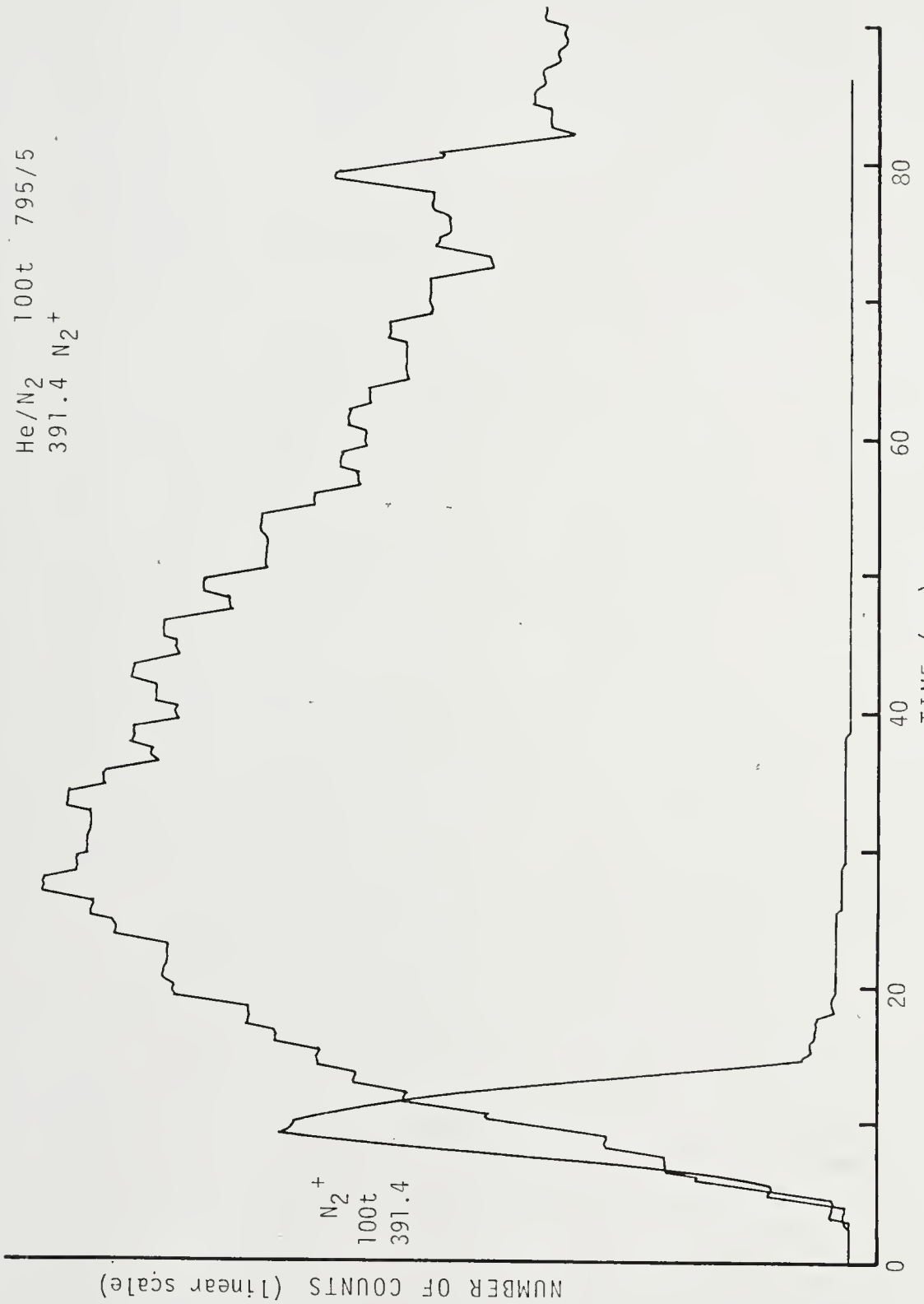

Figure 6. Metastable Transfer in He/N_2

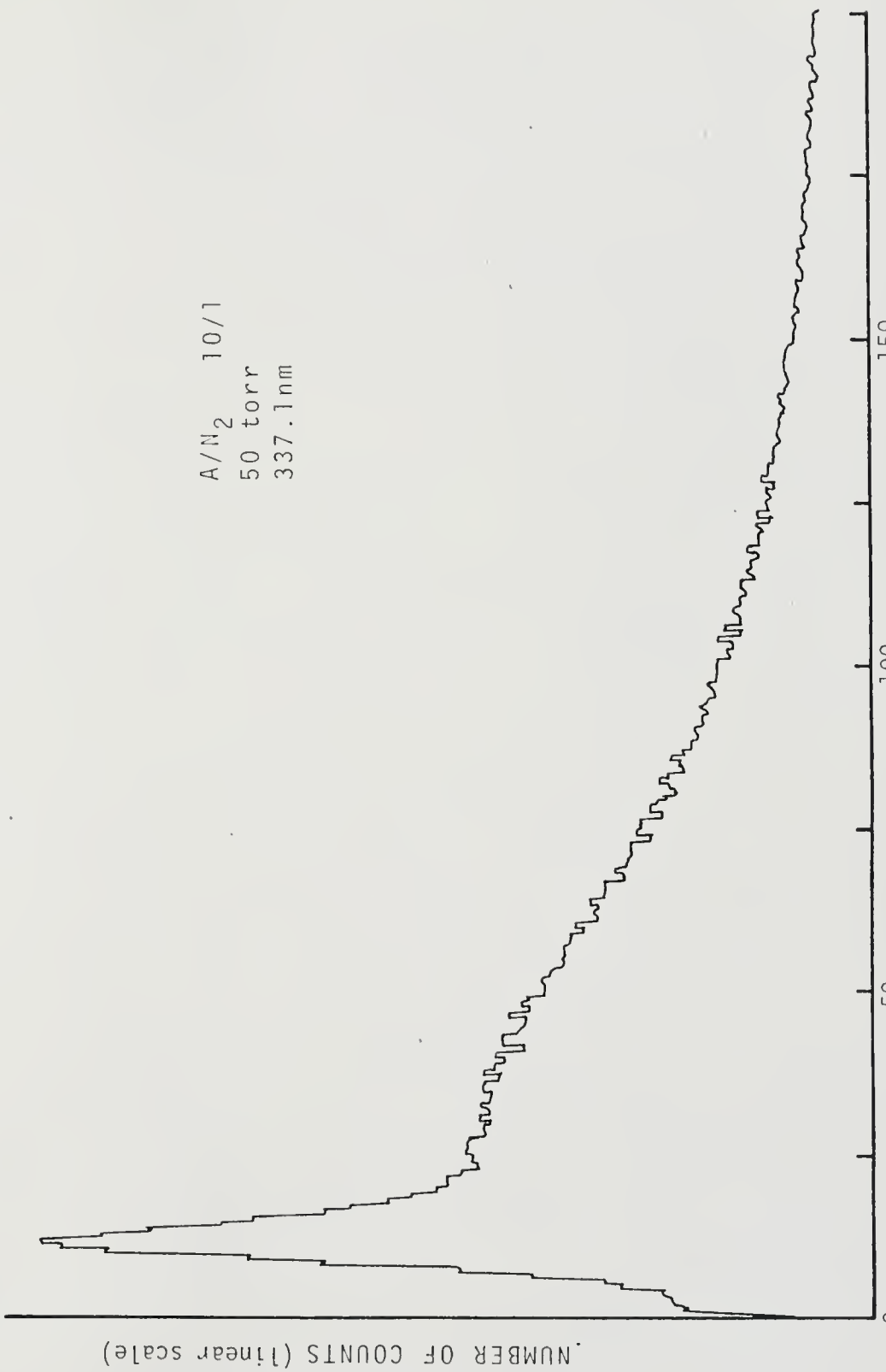

Figure 7. Double Decay Curve

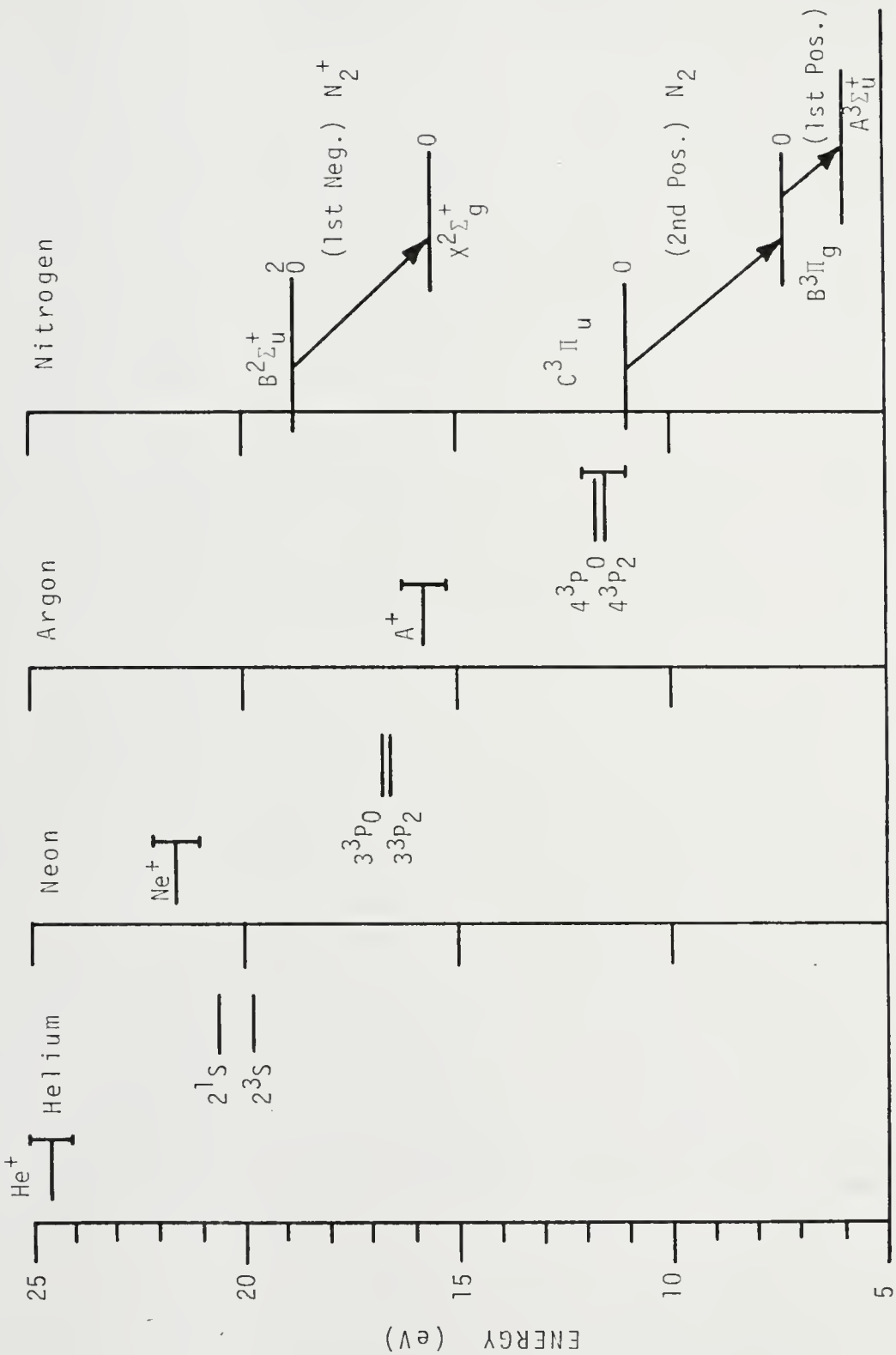

Figure 8. Relevant Energy Levels of He, Ne, A, and N_2

$B^2\Sigma_u^+$ level of N_2^+ and the metastable levels of helium and also the argon metastable, $C^3\Pi u$ resonance. These resonances lead to intense first negative and second positive emission respectively. By observing mixtures of the three inert gasses with nitrogen, we were thus able to examine the cases of neutral excitation (A/N_2), ion creation and excitation (He/N_2), and no interaction (Ne/N_2).

2.3 Rate Equation for $C^3\Pi u$

In this chapter we will confine ourselves to the relatively simple case of the $C^3\Pi u$ level of N_2 with no foreign gas present. For this restricted case, there was no cascading[8], metastable transfer or resonance trapping, and thus the rate equation is very simple, consisting of two deexcitation terms, collisional and radiative decay, and one excitation term, collisional excitation from the ground state. The collisional excitation "turns off" at t_f, the time at which the fission fragment left the observable region or had lost so much energy that it could no longer produce excited states. The rate equation thus separated in a very natural way into two parts, one before t_f, and one after.[5]

$$\frac{dN_2^*}{dt} = Q\frac{dE_d}{dt} - k_1N_2^* - k_2PN_2^* \qquad 0\leq t<t_f, \qquad (1)$$

$$\frac{dN_2^*}{dt} = k_1N_2^* - k_2PN_2^* \qquad t_f\leq t<\infty, \qquad (2)$$

where, N_2^* is the population of the $C^3\Pi u$ level, Q is the number of $C^3\Pi u$ states produced per unit energy deposited in the gas, E_d is the energy deposited by the fission

fragment, P is the pressure, t_f is the time at which the fission fragment collides with the wall or has slowed to the point where it can no longer cause excitation and ionization. k_1 and k_2 are the rate coefficients for the deexcitation reactions shown below:

$$N_2(C^3\Pi u) \xrightarrow{k_1} N_2(B^3\ u) + h\nu$$

$$N_2(C^3\Pi u) + N_2(X^1\Sigma g^+) \xrightarrow{k_2} \text{observed states.}$$

k_1 is the sum of all transition probabilities for the $C^3\Pi u$ state,

$$k_1 = A_{UL} = \frac{1}{\tau_r}\ \text{sec}^{-1},$$

where, τ_r is the radiative lifetime of the state, and k_2 is the two-body collisional quenching rate with units (sec^{-1} torr^{-1}).

After t_f, the population decreases monotonically, and Equation 2 may be solved to give

$$N_2^*(t) = N_{2\,max}^* e^{-(k_1+k_2P)t}. \qquad (3)$$

Solving the rate equations for $0 \leq t < t_f$ requires a functional form for the energy deposition of the fission fragment. While much has been written about the form of this function[9] [10], for nitrogen the energy deposition is adequately described by the square law for electronic stopping

$$E = E_0(1-r/R_e)^2, \quad \text{(See Appendix 1)} \qquad (4)$$

which, in terms of velocity is

$$v = v_0(1-r/R_e), \qquad (5)$$

where E and v are the energy and velocity of the fission fragment at the distance r from the source. E_0 and v_0 are

the initial energy and velocity of an average fission fragment. R_e is the extrapolated electronic range, $R_e = \frac{SRT}{PM}$, where S is the range in mg/cm^2; R is the gas constant; T the absolute temperature; P the gas pressure; and M the molecular weight of the gas. Integrating Equation 5 over the flight time and track length of the fission fragment gives

$$t_f = -\frac{R_e}{v_0} \ln(1-\frac{r_f}{R_e}). \qquad (6)$$

Solving Equations 3 and 6 together gives

$$\frac{dE_d}{} = ZE_0e^{-Zt} ,$$

where $Z = 2\ v_0/R_e$. Thus, for $0 \leq t < t_f$

$$N_2^*(t) = (\frac{ZE_0Q}{k_1+k_2P}) \{e^{-Zt}-e^{-(k_1+k_2P)t}\}. \qquad (7)$$

2.4 Relating Solutions to Observables

Since the intensity of I(t) equals $k_1N_2^*(t)$, determining the decay time of the intensity in the period $t_f \leq t < \infty$ gives the excited state lifetime directly. Since Equations 3 and 7 must be equal at t_f, $I_{max} = k_1N_{2max}^* = \frac{ZE_0Qk_1}{k_1+k_2P-Z}$ $\{e^{-(k_1+k_2P-Z)t_f}-1\}$. As τ goes to infinity, N_{2max}^* is just the total number of excited states produced by the passage of the fission fragment

$$N_{2max}^*(\tau\to\infty) = E_0Q(1-e^{-Zt_f}).$$

Integrating $k_1N_2^*(t)$ from 0 to ∞ gives the observable integrated intensity

$$I = \int_0^\infty k_1N_2^*(t)dt = k_1E_0Q\tau(1-e^{-Zt_f}).$$

Physically, N^*_{2max} is just the maximum excited state density that is obtained, and I is that fraction of the excited states which decay by radiation. Note that

$$I/\tau = I^*_{2max}(\tau\to\infty).$$

CHAPTER 3

SYSTEM AND CALIBRATION

3.1 Introduction and Design Criteria

The design of the experimental apparatus was determined in large part by the nature of the isotope source. The source emitted about 3000 fission fragments each second into the gas, and each fission fragment produced about 10^4-10^5 photons. Because of the very small solid angle subtended by the monochromator slit, it was expected that, on the average, one photon would be counted for each 1000 fission fragments. This extremely low light level demanded that single photon counting techniques be employed. Since thermally emitted electrons or dark counts could not be distinguished from single photons, the photomultiplier was cooled to decrease random background caused by thermionic emission of electrons from the photocathode. The key to the noise reduction and the advantage of this system over other single photon counting spectroscopy systems was the use of two photomultipliers in a delayed coincidence circuit which virtually eliminated the possibility of counting a random noise signal generated in only one of the tubes. The low flux level also required the ability to maintain suitable gas purity for the extended times necessary to establish acceptable statistics

(see Appendix 4).

The experimental apparatus (see Fig. 9) may be conveniently divided into three sections:

The experimental chamber,

The vacuum and gas handling system, and

The detection system.

The operation and calibration of each component section will first be described, followed by a discussion of system characteristics.

3.2 System Description

The experimental chamber was a 3.8cm i.d. double-sided Varian high vacuum flange. The side toward the total luminosity photomultiplier (TLP) had a pyrex window which was optically coupled to the TLP. The side facing the monochromator had a sapphaire window within 2mm of the entrance slit of the monochromator. The flange had two ports, one which connected with the gas handling and vacuum system, and the other through which the calibration source or high voltage electrode could be inserted. The ^{252}Cf source was cemented to the inside of the flange in such a way that a fission fragment emitted normal to the surface traveled along the long axis of the monochromator slit. In this way the light input to the monochromator was maximized.

The vacuum system was entirely stainless steel with copper gaskets. A combination of roughing, oil diffusion, and ion pumps were used to attain an ultimate vacuum of 5×10^{-9} mm Hg before filling with a test gas. The system was

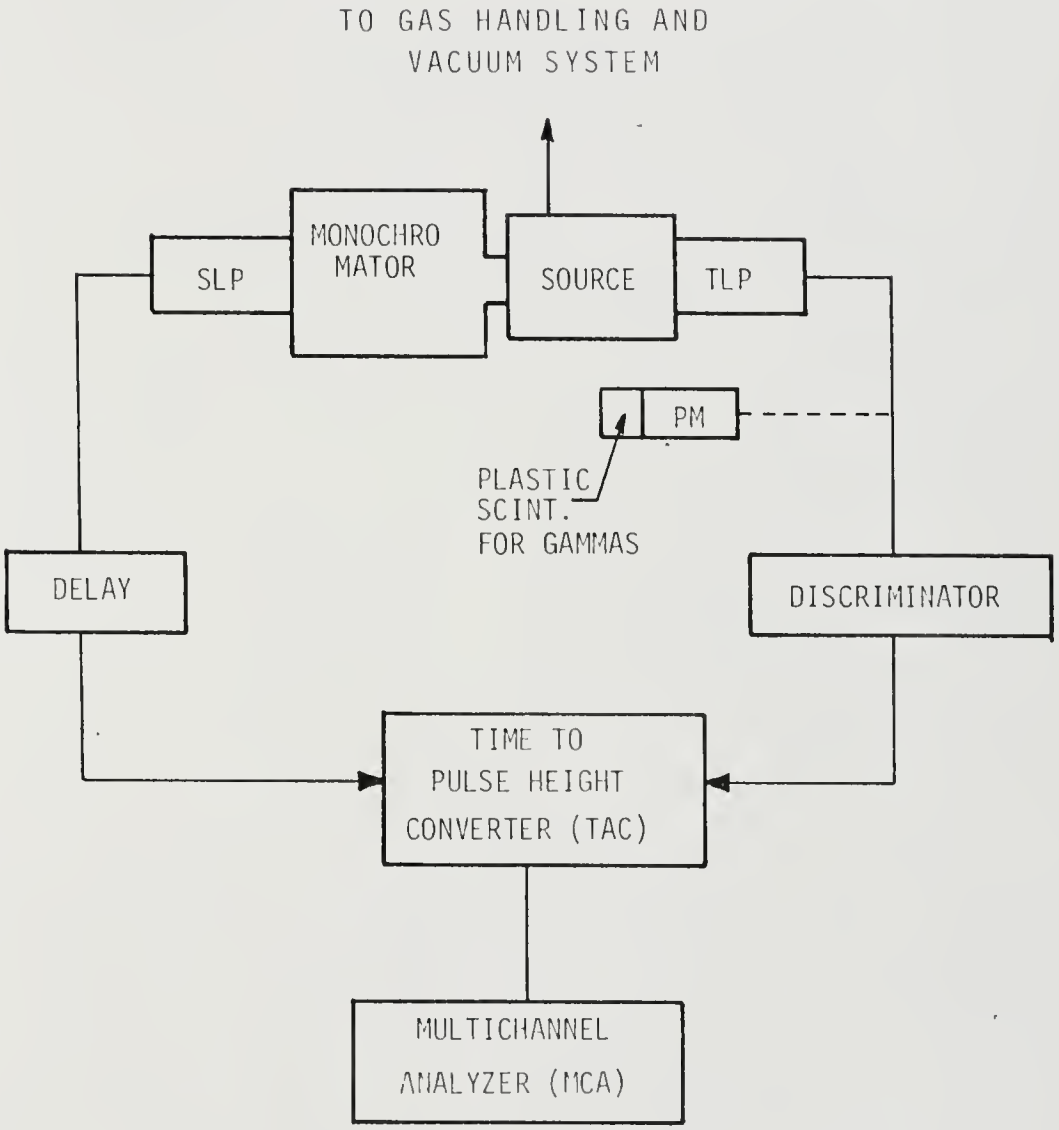

Figure 9. System for Lifetime Measurement

then filled with research grade gas and the pressure measured to within 1 torr with a Wallace and Tiernan gauge. Ultek high vacuum valves were used to completely isolate the system during the period of counting, which, in some cases, took as long as 72 hours.

The detection system may be described in terms of its four component functions:

a. Determine when a fission fragment has passed through and excited the gas (the total luminosity photomultiplier, TLP).

b. Determine when an excited atom or molecule has decayed by the emission of a photon (the specific luminosity photomultiplier, SLP).

c. Measure the time interval between the excitation and decay (the time to amplitude converter, TAC).

d. Digitize, accumulate and store measurements for successive fission fragments (the multichannel analyzer, MCA).

a. When the fission fragment passed through the gas, a large burst of photons was produced. These photons were of all wavelengths and were spread in time between the fission and the final decay of the longest lived of the atomic and molecular states which, in some cases, could involve times as long as 80 microseconds. When these photons struck the photocathode of the TLP, they produced

a current pulse which triggered a built-in discriminator. The discriminator, which used zero crossover timing, generated a fast negative logic pulse when half the total charge had been collected. To use this signal for timing, it was necessary to know how it was related in time to the fission event. This time relationship was determined in the following manner. Within 10^{-11} seconds of fission, a burst of prompt gamma rays occurred and was detected by a fast plastic scintillator mounted on a photomultiplier placed underneath the experimental chamber. The time interval between the gamma burst or fission and the peak of the total luminosity pulse was thus determined (see Appendix 2). In addition, the lifetime of an excited state was measured using first the gamma detector and then the TLP to start the timing (see Appendix 3). The measured lifetimes in both cases were found to be identical. Thus, the output of the TLP was related to the time of fission and, hence, to the time of excitation by a fixed and known time lag.

b. The photons from the gas passed through a sapphire window and into the entrance slit of the monochromator. Because of the close proximity of the monochromator slit to the source, no system of lenses would have increased the light input. The monochromator was a Model 218, 0.3 meter focal length Czerney-Turner, manufactured by the McPherson Instrument Corporation, with the grating blazed for 300nm. Mounted directly behind the exit slit was an RCA 8575

photomultiplier contained within a thermo-electrically cooled housing. The system was calibrated for relative wavelength sensitivity using an Eppley Tungsten filament lamp certified by NBS. No absolute calibration was attempted. The output of the anode was dropped across a 50 ohm load resistor to give fast time response and the resulting pulse sent to an Ortec Model 260 time pickoff unit. The time pickoff unit consisted of a pulse transformer, a wide-band transitor amplifier, a tunnel diode discriminator, and a line drive buffer. The unit acted essentially as a fast, low level timing discriminator. When an input pulse exceeded the discriminator setting, a NIM standard fast negative logic pulse was generated.

c. The time-to-amplitude converter measured the time interval between the leading edges of logic pulses furnished to its start and stop inputs and generated an analog output pulse that was proportional to the measured time interval. The start pulse initiated the charging of a highly linear capacitor, and the stop pulse terminated the charging. The voltage across the capacitor was thus proportional to the time interval between the two signals and served as the output. Since the TAC was triggered by the leading edge of the input pulse, it was necessary for good time resolution that the pulses have very fast rise times and that they exhibit a small dynamic range. These criteria were statisfied by using NIM-standard fast negative logic pulses. The start pulse was supplied by a zero crossover

discriminator built into the base of the TLP, an Ortec Model 264 photomultiplier timing discriminator and preamplifier. This unit also provided a linear or analog output which was used in conjuction with an Ortec Model 410 linear amplifier to set the discriminator level above the alpha particle peaks so that the system responded only to the fission fragments. Since both the TLP and the SLP were responding to photons produced at about the same time, the pulses from the SLP were delayed by a nanosecond delay unit to allow time for the zero crossover discriminator in the TLP to determine the time of fission. The arrival of the start pulse opened a time window whose width could be set from 50 to 80,000 nanoseconds. During this time window, a photon hitting the photocathode could stop the TAC, thereby producing an output pulse. If no photon was received before the end of the time window, the TAC automatically reset and was then ready to receive another start pulse. The fraction of start pulses which were followed by a stop pulse was thus related to the number of photons present in the experimental chamber. The detailed behavior of the number of true stops as a function of time accurately reflected the time decay of the photon density and, thus, the population of the excited level.

d. The output of the TAC was sent to a TMC Corporation multichannel analyser (MCA). Using a Model 210 pulse height logic unit, the height of each output pulse from the TAC was measured and sent to a channel whose address cor-

responded to the measured pulse height and, thus, to the measured time-after-fission. Counts were accumulated for a period of time determined by the arrival rate of photons at the SLP. The fewer photons per second being counted, the longer the measurement had to be made in order to accumulate adequate statistics. The period of counting could be varied from five minutes up to 72 hours, the upper limit being set by the necessity for maintaining adequate gas purity (see Appendix 4). After measurement was completed, the contents of the MCA memory was read out to an X-Y plotter for qualitative analysis and the digital values punched on paper tape for subsequent computer analysis.

3.3 Calibration

To determine the minimum decay time that this system could measure, a small chip of an "ultra fast" plastic scintillator (NE-111) was suspended in the middle of the excitation region (see Appendix 2). The measured decay time of 1.67±.06ns showed no broadening compared with the published value of 1.7 ns. Since no scintillator could be found with a shorter decay time, the minimum that this system could measure is still unknown. The TAC was capable of resolving signals 10ps apart. The system was ultimately limited by the photomultipliers which have rise times on the order of 1ns.

The minimum resolution in a real experiment is limited generally by the statistical accuracy of the number of counts which can be measured in the time over which condi-

tions may be expected to remain unchanged. To determine the variation due to counting statistics and errors associated with filling the system to a chosen pressure, decay measurements at two different pressures were repeated ten times each. The standard deviation of what should be identical measurements was 0.138ns at 800 torr and 0.324ns at 100 torr, or about 4% in each case.

Identification and elimination of the gamma background proved to be a major experimental difficulty. In our previous experiments in the reactor, signal noise caused by gamma rays striking the photomultiplier had required extensive shielding, a massive low-pass filter, and extremely slow scanning speeds. The original reason for considering a coincidence system was the freedom it seemed to offer from gamma background. Since the gammas are discrete particles, and thus capable of striking only one photomultiplier at a time, requiring coincidence between the outputs of the photomultipliers should have eliminated the possibility of responding to gamma noise. Examination of early decay curves, however, showed a peak occurring shortly after fission which was finally traced to a coincidence between the fission fragment signal from the TLP and a gamma noise pulse in the SLP. Because the prompt gammas, unlike decay gammas, do not occur at random but are emitted within 10^{-11} seconds of fission, coincidence does occur between the fission fragment and the gammas (see Fig. 2). These gamma pulses were thought to be due to ionization of the residual

gases within the tube and to scintillation of the quartz window. The background level was found to be greatly increased by opening the system and exposing the photomultipliers to light, even with no voltage applied. After such an exposure, about six hours was required before the background level approached steady state. Extensive tests were made to determine how the signal to noise ratio changed with photomultiplier voltage. The signal to noise ratio was found to increase monotonically as the high voltage was reduced. If the voltage was reduced too much, however, the fission fragment could not be distinguished from the alpha particles. The optimum situation was when the voltage of the two photomultipliers was the same and equal to 2200 volts.

3.4 Output

After a lifetime measurement had been completed, the data was in the form of integer values between zero and 2^{20} located in the memory of the MCA. Each channel corresponded to a time interval determined by the full scale setting of the TAC. For example, system calibration showed that when the full scale setting of the TAC was 50ns and 64 channels of the MCA were being addressed, 10ns covered a range of 12 channels. Thus, each channel corresponded to 0.83±.04ns. The channel by channel accumulated count was read out along with the corresponding channel number either in analog form onto an X-Y plotter, in decimal form on adding machine tape, or punched in binary coded hexidecimal on paper tape. In practice, the data was always

displayed in analog X-Y form for quick analysis. If the data appeared to be of interest, it was punched on paper tape and the paper tape later read into the IBM 1800 computer and stored in a file on a magnetic disk. This data was then available for immediate analysis and future reanalysis.

3.5 Scanning Mode

The system was also capable of being used as a very sensitive scanning spectroscopic system (see Fig. 10). To scan, the system was set to respond to all photons of the correct wavelength regardless of the time of occurrence and then to step the spectrograph and a counter simultaneously so that the number of photons at each wavelength was counted. In this mode of operation, the time window of the TAC was set wide enough to include the entire decay curve of the excited level. Any photon of the correct wavelength that was associated with a fission fragment thus gave rise to an output pulse. Using the internal single channel analyzer (SCA), this output pulse was converted into a NIM standard 5-volt slow logic pulse and supplied to the input of a multiscaler logic unit in the MCA. The multiscaler unit addressed each channel of the MCA sequentially and stepped when it received a trigger pulse. This trigger pulse was supplied by a recycling timer which would supply trigger pulses with any chosen interval. This trigger pulse was also supplied to a stepping motor connected to the wavelength drive of the

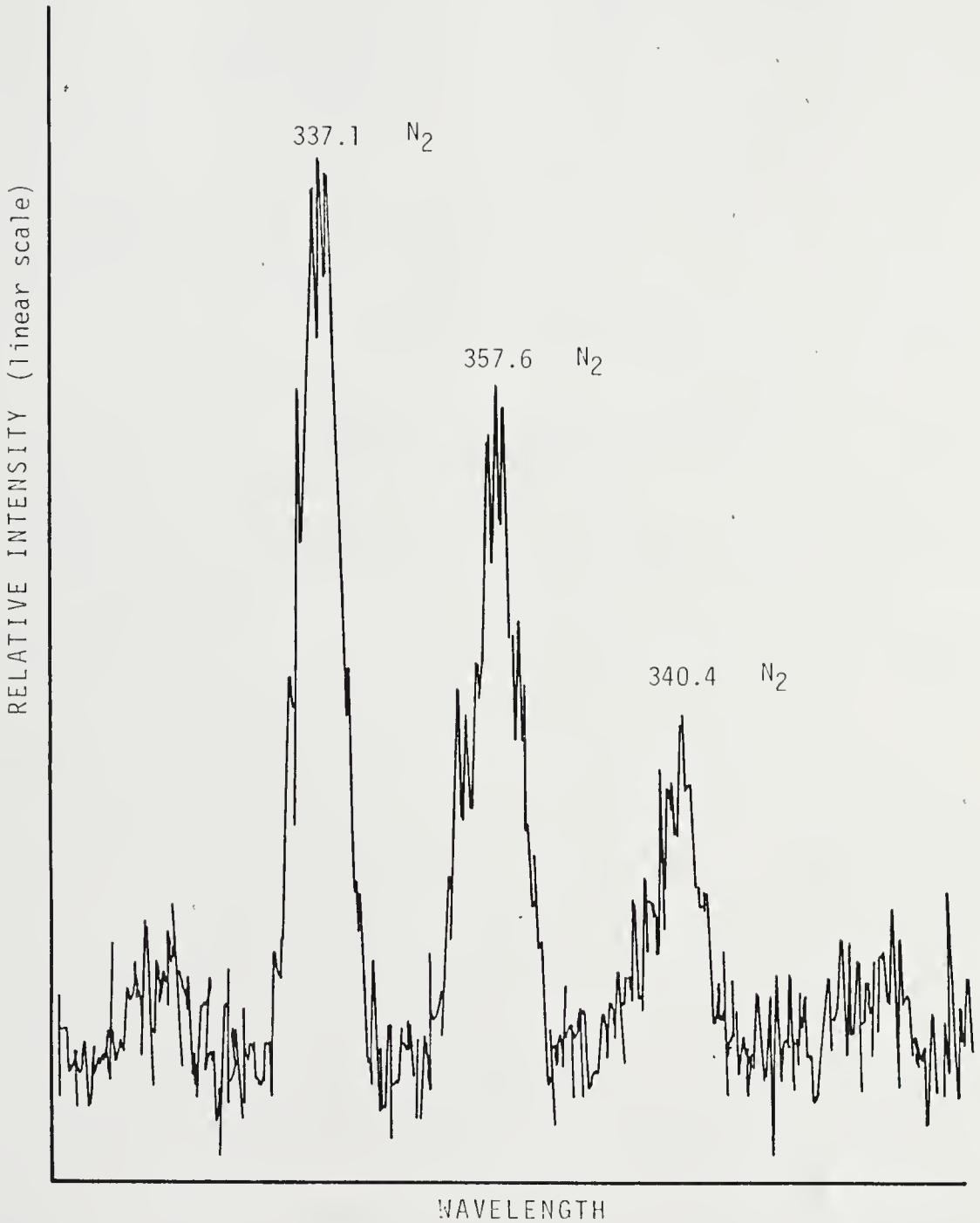

Figure 10. Scan of Pure N_2

spectrograph and served to step the spectrograph and multi-scaler simultaneously. Because of the wide slits on the spectrograph, it was found to be sufficient to sample the intensity every 0.2nm corresponding to 46 steps of the stepping motor for each trigger pulse. The length of time counted at each wavelength varied with the intensity of the light. When scanning a gas, such as an argon-nitrogen mixture which is very bright, 10 seconds per channel proved sufficient while for some poor emitters, several hours at each channel were necessary.

An interesting feature of this mode of operation was the ability to make a scan at any point in time. That is, by setting the TAC to respond only to photons which occurred between, say, 10 and 18ns after fission, we had a spectrograph with an 8ns shutter which opened 10ns after fission (see Fig. 35). A spectral scan at several times after fission could provide a complete time history of the intensity at all wavelengths.

CHAPTER 4

ANALYSIS AND RESULTS

4.1 Introduction

The basic question addressed in this chapter is that of relating the raw data to the fundamental properties of the fission fragment excited gas. How the system characteristics affected the raw data was discussed in Chapter 3. Here we shall assume that the value of N(t) has been corrected for instrumental influence and try to determine how these values relate to the radiative and collisional decay coefficients. We shall first discuss how the computer programs processed the raw data and then proceed to a detailed discussion of the four output parameters τ, N(t), $SUMN_i$, N_{max}, and their interpretations (see Fig. 1). Finally, some consideration will be given to general problems relating to any measurement carried out with this system.

4.2 Programs

After an experiment had been performed and a count completed, the data was stored in the memory of the MCA. This data was immediately punched in hexadecimal form onto paper tape and then read into an IBM 1800 computer and placed in a file on a magnetic disk. All the data and the current working programs were kept on this disk and, together with the lab book, provided a complete record of the

experiment. Once the data was on the disk, there were two programs which could be called upon for analysis: $SUMN_i$ which printed the sum total of counts between any chosen limits thereby giving a number proportional to the number of excited states which decayed by radiation in the time interval specified, and SLOGP.

SLOGP first plotted $\log N_i$, the log of the number of counts, versus the channel number i. Since the decay curve was expected to be a simple exponential decay, the SLOGP plot was visually examined to determine if there was a straight line region and, if so, what channels comprised it. In addition, this plot allowed a good determination of just where background occurred. Once the limits of the decay region had been determined, the program performed a least squares fit of the experimental data to an equation of the form $Y_i = Ae^{-ti/\tau}+B$ in the region chosen from the log plot and specified by the operator. The operator supplied an initial value of background chosen to be just below the value obtained from the log plot. An iterative calculation was then performed for the number of iterations and with the iteration interval specified by the operator. For each value of the background, a least squares fit was made and the value of the error function calculated. After the iteration was complete, the value of background for which the error function was a minimum was chosen, and both the raw data and the chosen fit were plotted along with the numerical values for A, τ, B, and the error function. If

the fit appeared to be flawed, new values of starting channel, stopping channel and background could be chosen and a new curve superimposed upon the old for comparison.

4.3 Analysis

Once the data had been analyzed by the programs, there were four numbers available:

1. τ, the time it took for the excited state population to decrease by a factor of 1/e.
2. N(t), proportional to the number of excited states decaying at time t.
3. $SUMN_i$, proportional to the number of excited states which decayed between the time A and the time B.
4. N_{max}, proportional to the greatest emission rate.

The decay time determined by the least squares fit of the raw data was the sum of the radiative and collisional decay times. Since the radiative decay time is an atomic constant, while the collisional decay time changes with pressure, it is possible to determine the two effects separately. As the pressure decreased, collisions became less frequent, and the collisional decay rate decreased until at zero pressure, the decay of the excited states was entirely determined by the radiative decay.

The decay time τ is equal to $1/(k_1+k_2P)$, so that by plotting $1/\tau$ versus pressure, the data should fit a straight line with an intercept k_1 and a slope k_2. Deviation from a

straight line, indicating nonlinear behavior, was observed at the highest pressure studied (800 torr). This deviation indicated that three-body collisions were becoming important and any studies carried out at this pressure or greater should include a quadratic pressure term in the rate equation. Figure 5 shows the results for the $C^3\Pi u$ level of pure nitrogen with the determined values of k_1 and k_2 shown. This curve represents the analysis of 82 decay time measurements.

There were three sources of difficulty which may cause errors in the interpretation of the lifetime curves. These three problems all took the form of additional excitation terms in the rate equation other than direct excitation, some of which persisted sufficiently late in time that there is no true "decay" period.

Resonance trapping will cause the population of a level connected to the ground state by an optically allowed transition to be maintained at an artificially high level compared with the optically thin case. The two most satisfying solutions to this problem are either to solve the equation of radiative transfer simultaneously with the rate equations or to choose a level for which there is no radiation trapping.

Cascading causes the population of an intermediate level to continue to be augmented by the decay of higher lying levels for some time after the end of the excitation pulse. This problem may be solved by either solving the

coupled sets of rate equations for all the levels in the gas or by choosing a level which has no significant cascade contributions.

Collisional transfer between excited levels in a decaying gas causes an irreversible flow of excitation energy toward the lowest excited state within a closely spaced group of levels. The collisional transfer rate, and hence, the collisional quenching coefficient, is explicitly solved for in this dissertation.

It should be noted that one source of uncertainty usually present in plasma spectroscopic diagnostics was avoided here. No assumptions about equilibrium or departures therefrom were necessary. The measurement of the decay time was independent of the relative populations of the various levels subject to the three preceding cautions. In fact, one could hardly imagine a more nonequilibrium gas either spatially or temporally than that being presently considered.

The curves of intensity versus time yielded the temporal variation of the population. It may be noted that this variation was in fact the solution of the rate equations for the particular level observed. The rise time of the population was nearly constant for all levels in all gases at all pressures, and this surprising result is discussed at more length in Appendix 5.

Plotting N_{max} versus pressure (Fig. 11) we find that the maximum excited state density occurred at about 350 torr but did not exhibit a particularly sharp maximum.

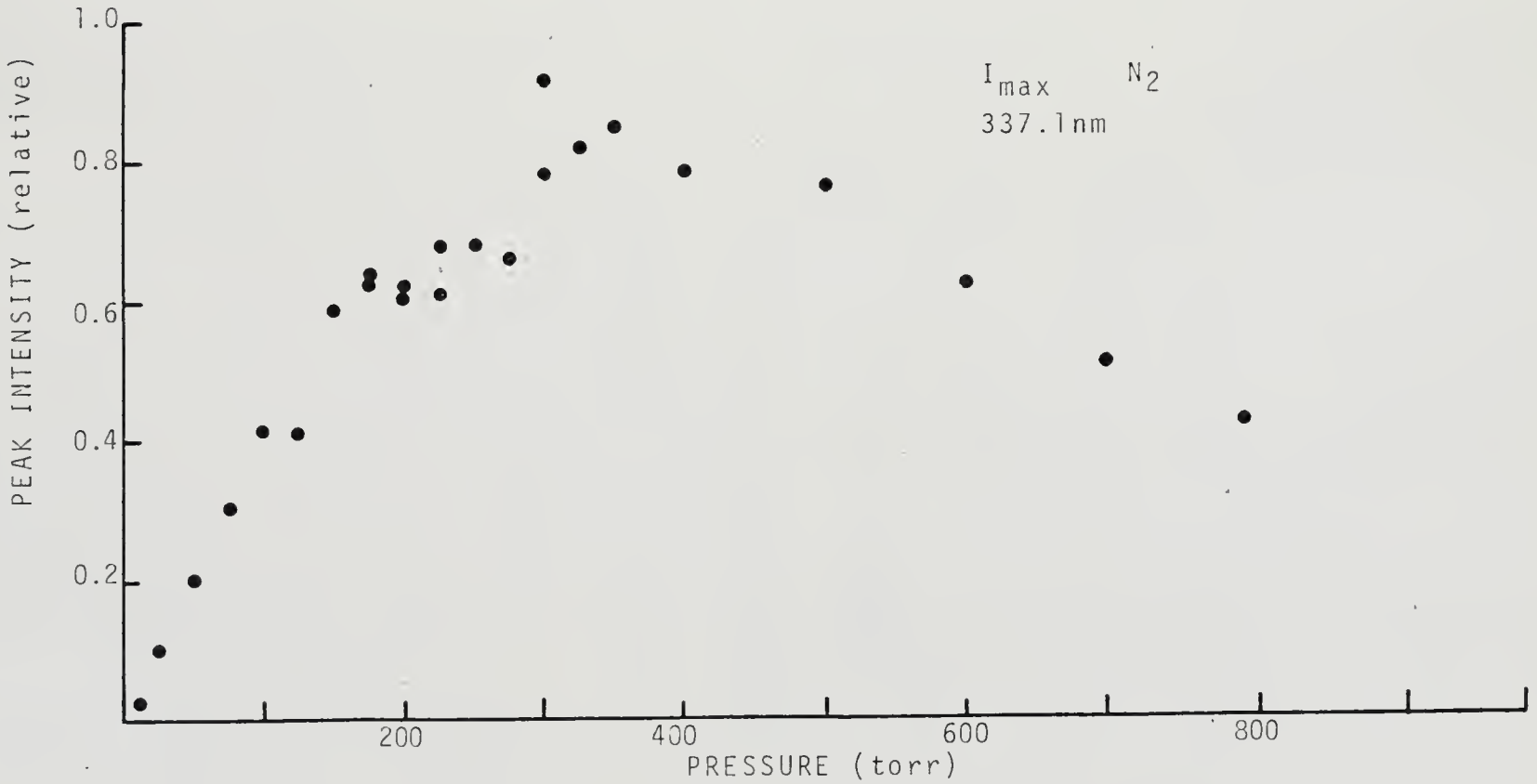

Figure 11. Peak Intensity Versus Pressure for 337.1nm

From Section 3 we see that SUMN/τ plotted against pressure should show identical behavior which, in fact, it does (see Fig. 12).

As shown in Section 3, the sum of the counts in all channels can be related to the ratio of the radiative decay constant and the collisional decay constant. Alternatively, if k_1 and k_2 are known from the decay curve, SUMN can be related to the total number of excited states created by the fission fragment passing through the gas, $QE_0(1-e^{-Zt_f})$. Figure 13 shows the variation of the integrated intensity with pressure. The curve indicates a rather narrow peak occurring at about 175 torr. Comparing Figures 11 and 13, we may observe that a pulsed laser might operate best at a different pressure than would a CW laser. Since, in the pulsed case, we are interested in the greatest instantaneous population, we would choose the peak in Figure 11, while for the steady state case, we are concerned with the average population density and would follow Curve 13.

4.4 Pulse Height Distribution

One tremendous advantage to using the decay curve for determining the lifetime or transition probability of an excited state was that it didn't depend upon the number of excited states created, but rather upon how those that were created changed with time. What was being measured then was not intensity, but the rate of change of intensity which was much easier to do. The number of excited states created by the passage of a fission fragment was propor-

Figure 12. Integrated Intensity Divided by Decay Time as a Function of Pressure

Figure 13. Integrated Intensity Versus Pressure

tional to the energy deposited which was, in turn, dependent upon the initial or birth energy of the fission fragment. Fission fragments at birth showed a distribution of energies divided into two rather well defined groups. The energy distribution of the ^{252}Cf source used in the experiment, measured with a surface barrier detector, is shown in Figure 14. Since some fission fragments have a greater initial energy than others, they will, on the average, create more excited states in passing through the gas. Thus, the intensity we observed after the passage of a fission fragment was dependent to some extent upon the particular particle we chose to observe. Note, however, the rate at which the excited states died away did not depend on the energy of the fission fragment which created them. Looking at the output of the TLP, the amplitude of the total luminosity pulse was proportional to the number of photons resulting from the passage of the fission fragment. At constant pressure, this was proportional to the energy of the incident particle.

The pulse height distribution in the gas is shown in Figure 15. This distribution was measured in CF_4, a gas which gives a large number of photons per unit energy deposited and, hence, provided good scintillator resolution.

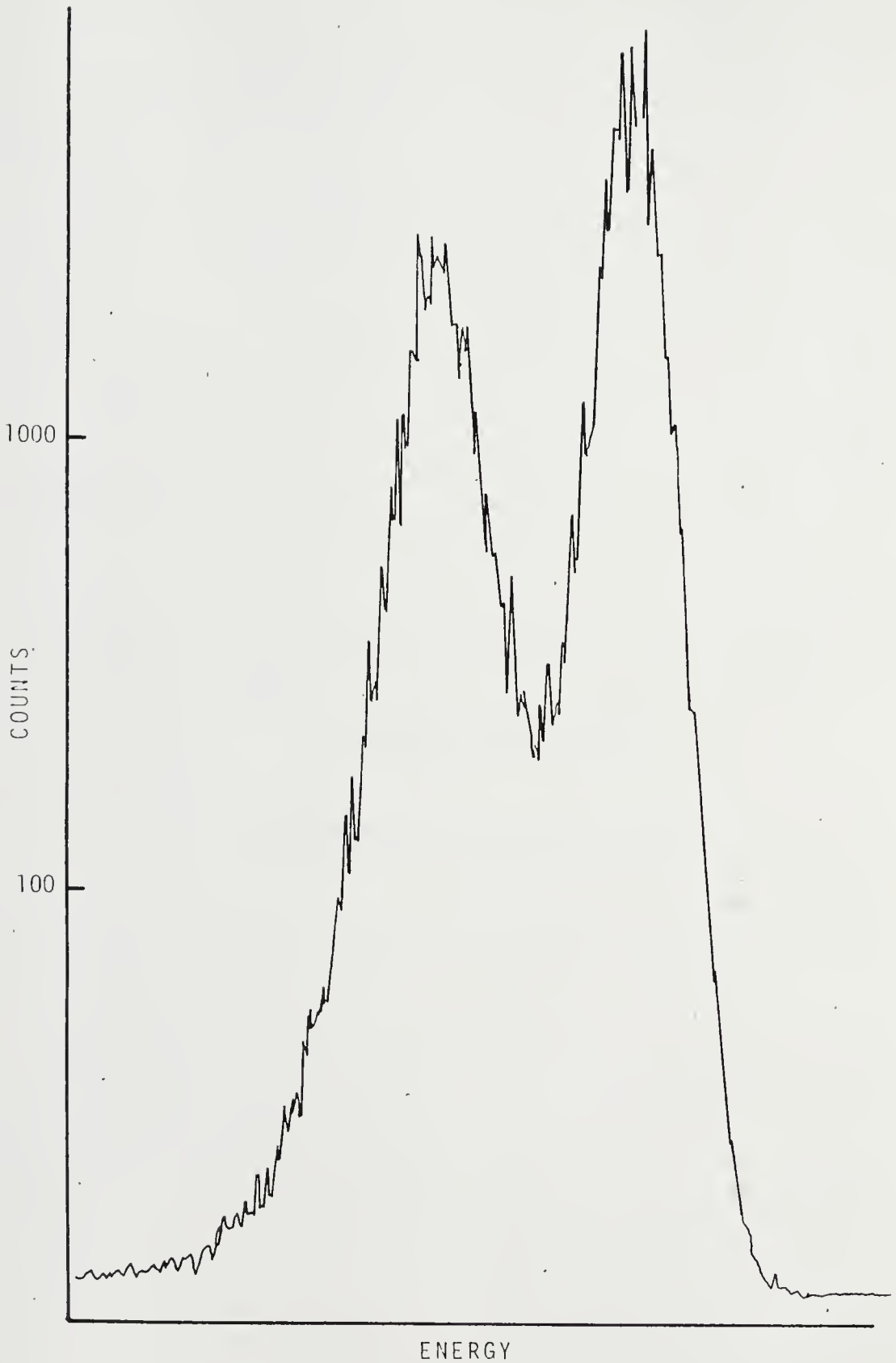

Figure 14. Fission Fragment Energy Spectrum

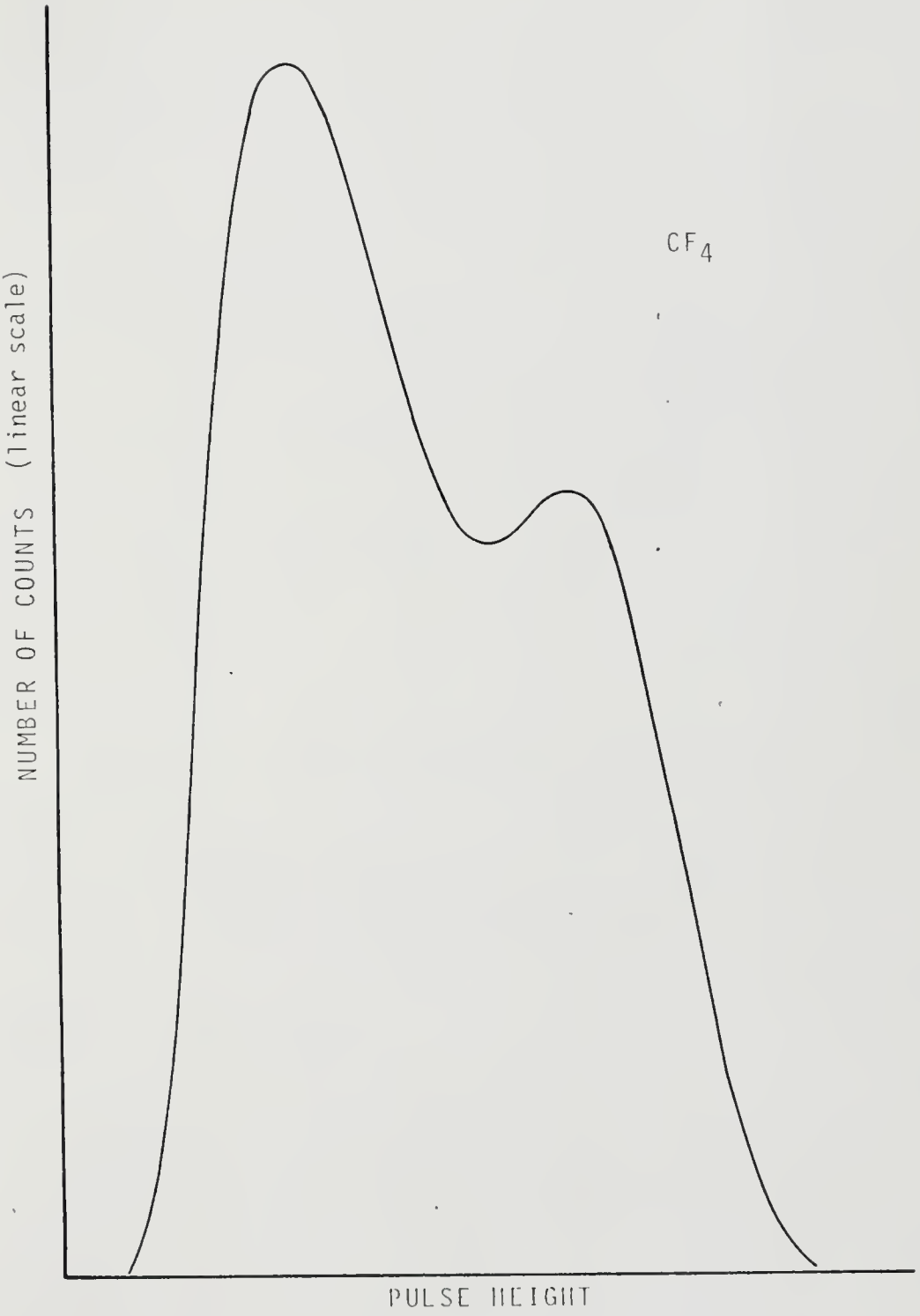

Figure 15. Fission Fragment Distribution from TLP Pulse Heights

CHAPTER 5

OTHER GASES AND GAS MIXTURES

5.1 General Comparison of Mixture Spectra

Figure 16 shows scans of the fission fragment excited nitrogen impurity spectrum of one atmosphere neon, argon, and helium alongside that of pure nitrogen. Notice that the argon and helium were scanned five times faster than the neon and nitrogen, and hence, their peak heights or intensities should be increased by a factor of five for direct comparison. That the nitrogen impurity in argon and helium was so much brighter than either pure nitrogen or nitrogen in neon, was a consequence of the efficient transfer of energy from the metastable energy traps in argon and helium in to nitrogen. The dominant emission from helium was the 391.4nm N_2 band, while that from argon was in the 337.1nm N_2 band, both of which results follow immediately from a consideration of Figure 8. The dominant emission from neon was also the 391.4nm band, and this has not been explained. The relative peak heights adjusted for the different scan speeds of the most intense emission from each gas goes as neon to argon to helium to nitrogen,

$$2.1 : 1.3 : 13.7 : 1 .$$

5.2 Neon/Nitrogen Mixtures

Besides the measurement of the decay time of the $C^3\Pi u$

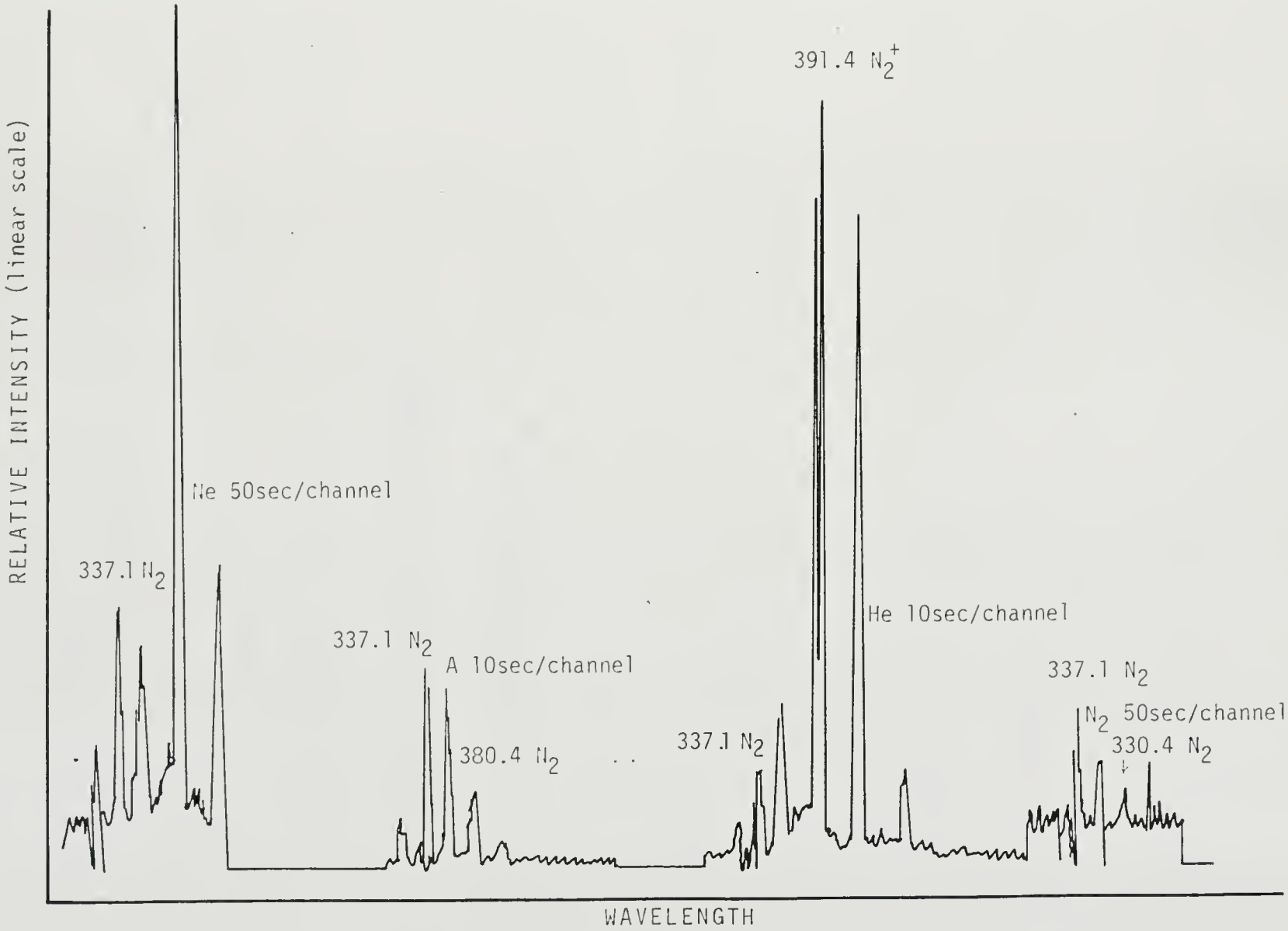

Figure 16. Scans of Nitrogen Impurities Ne, A, He, and Pure N_2

state of nitrogen, several other studies were carried out to illustrate the versatility of the system for the study of fission fragment excited gases. An extensive study was made of neon and neon-nitrogen mixtures. Using this mixture provided the opportunity of viewing, simultaneously, three lines from three different species, atomic neon, molecular nitrogen, and the nitrogen molecular ion. Figure 17 is a spectral scan of fission fragment excited neon showing the nitrogen impurity emission. Looking first at the 585.2nm neon line in pure neon, we find a radiative lifetime of 16.6±.7nm (see Fig. 18). As the nitrogen impurity concentration increased from 1% to 10% to 50% (Figs. 19, 20, 21), there was no significant change in the lifetime of the neon excited state. This might be expected since there was a very poor energy match between the levels of neon and those of nitrogen. The values for k_2, the collisional transfer coefficient, appeared to show a systematic decrease with nitrogen concentration. If this trend is real, it means that the nitrogen is less effective than the neon in quenching the level that gives rise to the 585.2nm line. Looking next at the $C^3\Pi u$ level of nitrogen with neon concentration values of 1%, 10%, 90%, and 99% (Figs. 22, 23, 24, 25), we see that when the nitrogen was the dominant gas, the lifetime varied strongly with pressure; whereas, when the neon was dominant, there was very little change. This again tells us that there was not much interaction between the levels of the two gases.

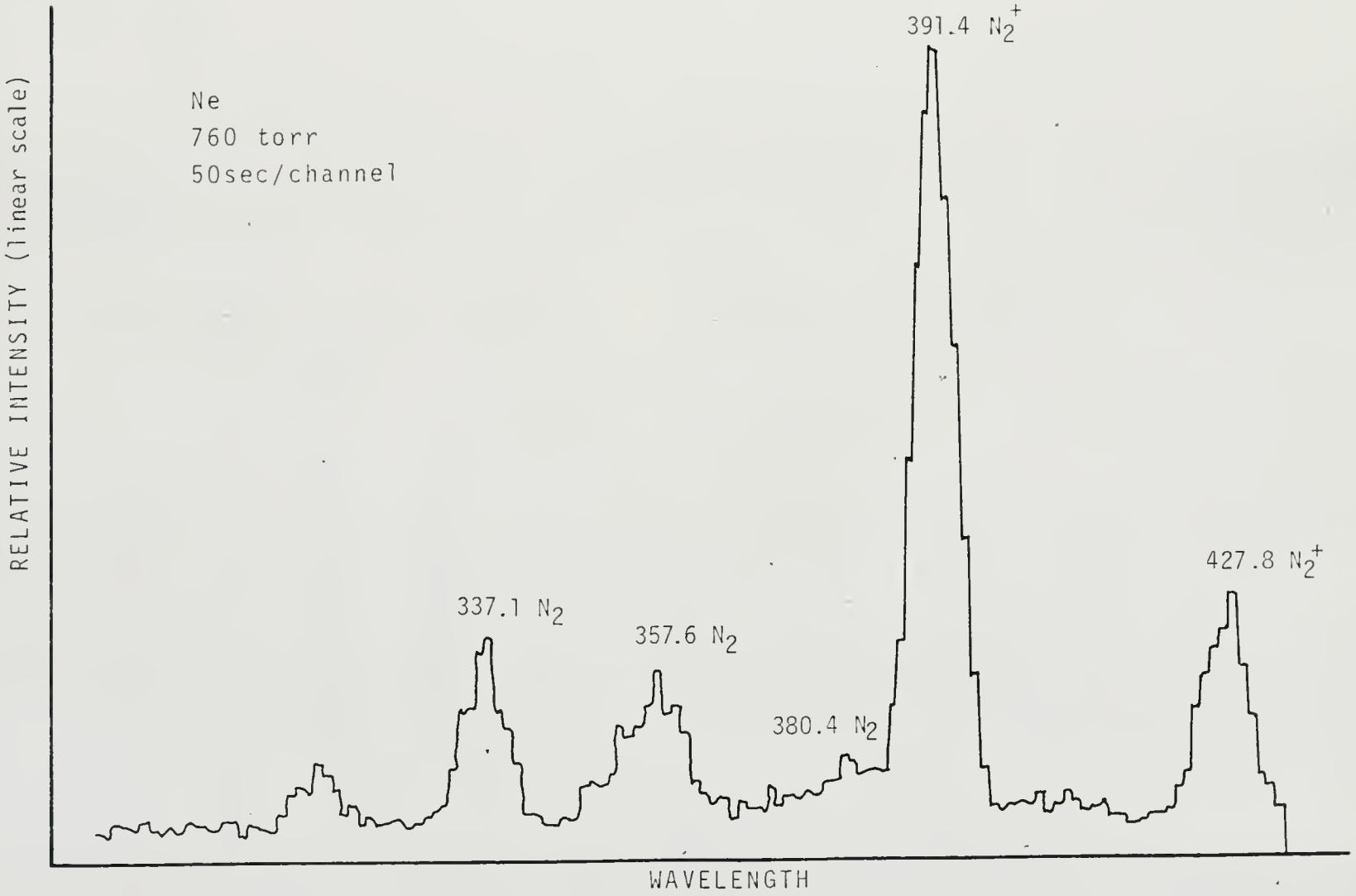

Figure 17. Scan of Nitrogen Impurity in Pure Neon

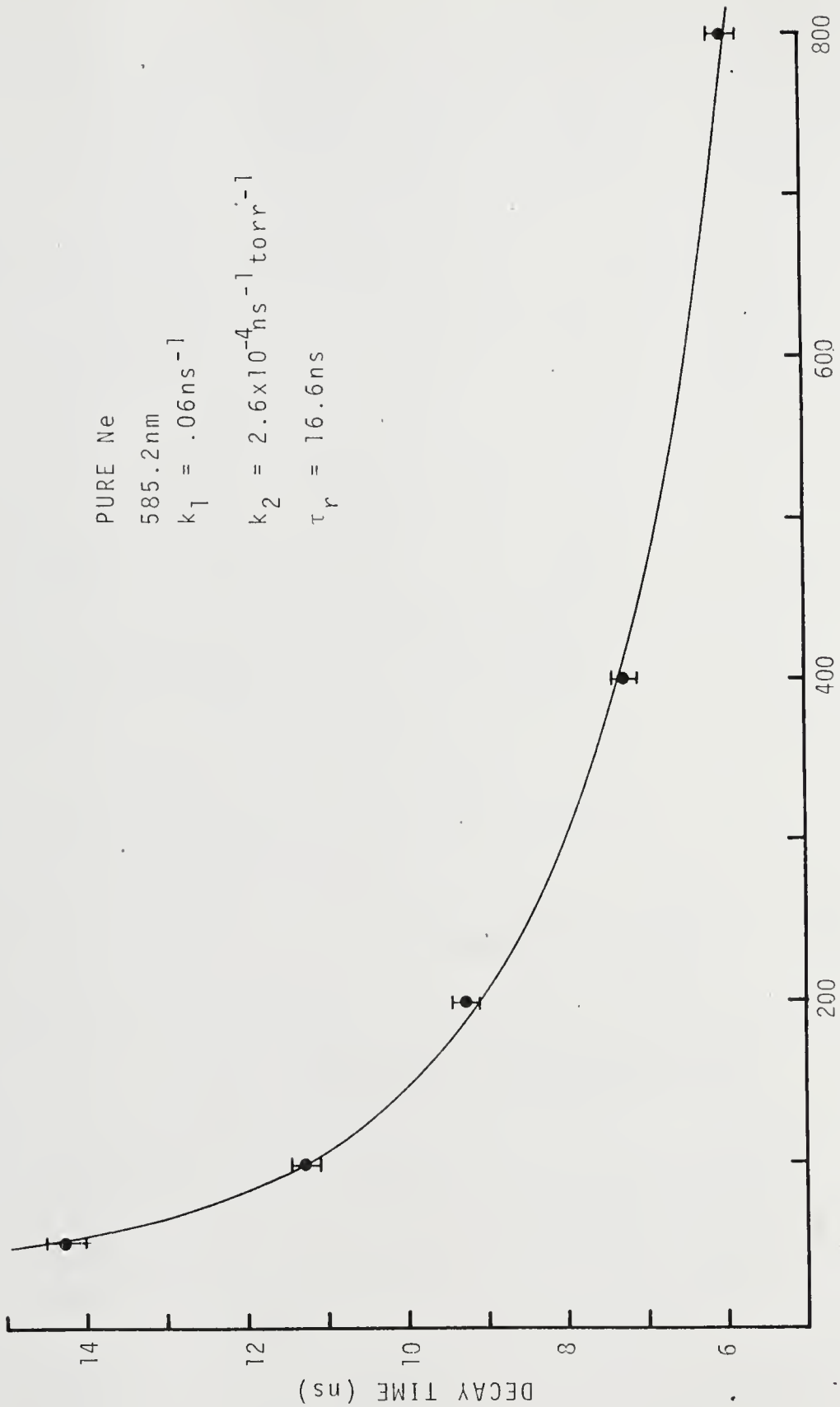

Figure 18. Decay Time Versus Pressure for 585.2nm

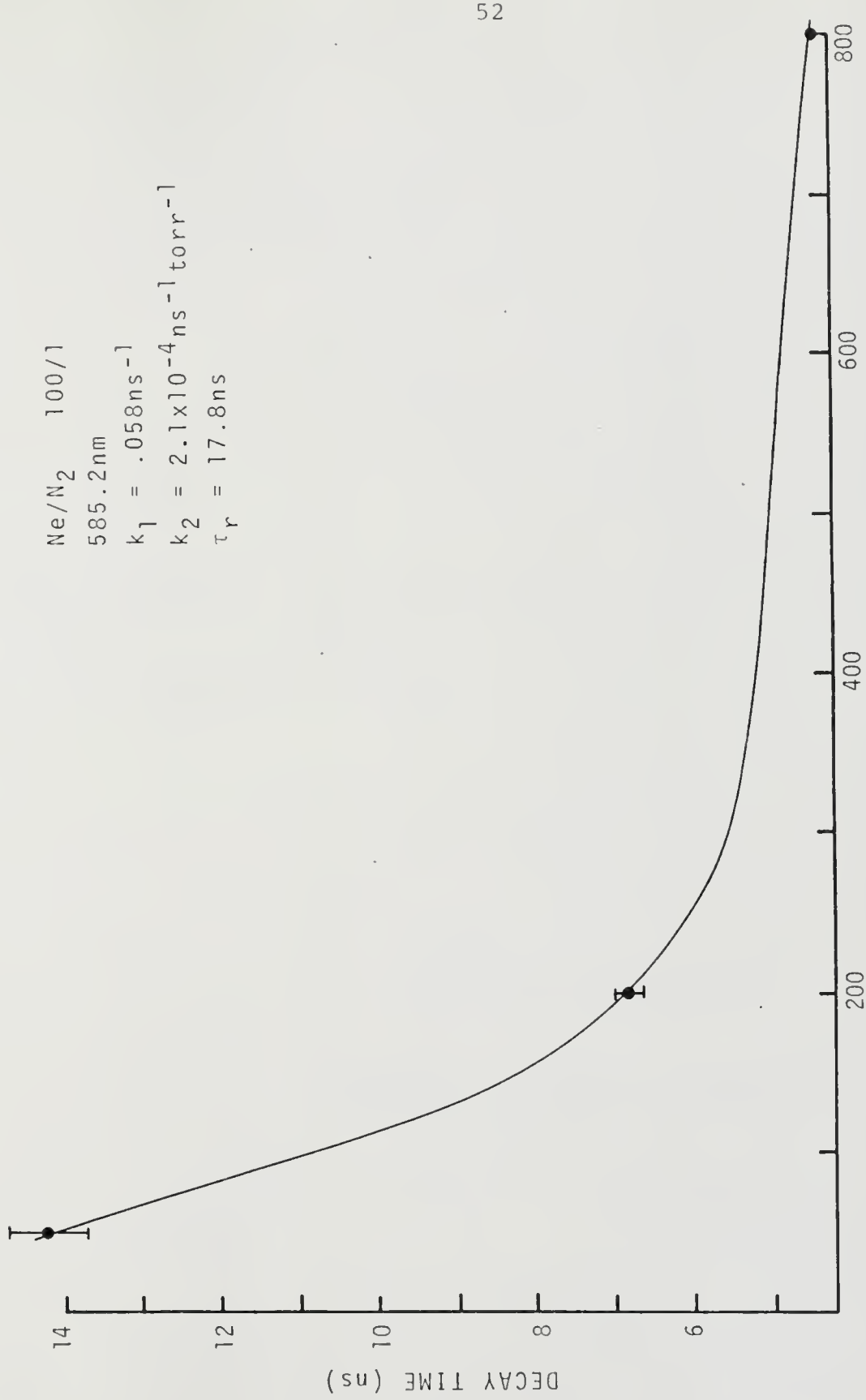

Figure 19. Decay Time Versus Pressure for 585.2nm

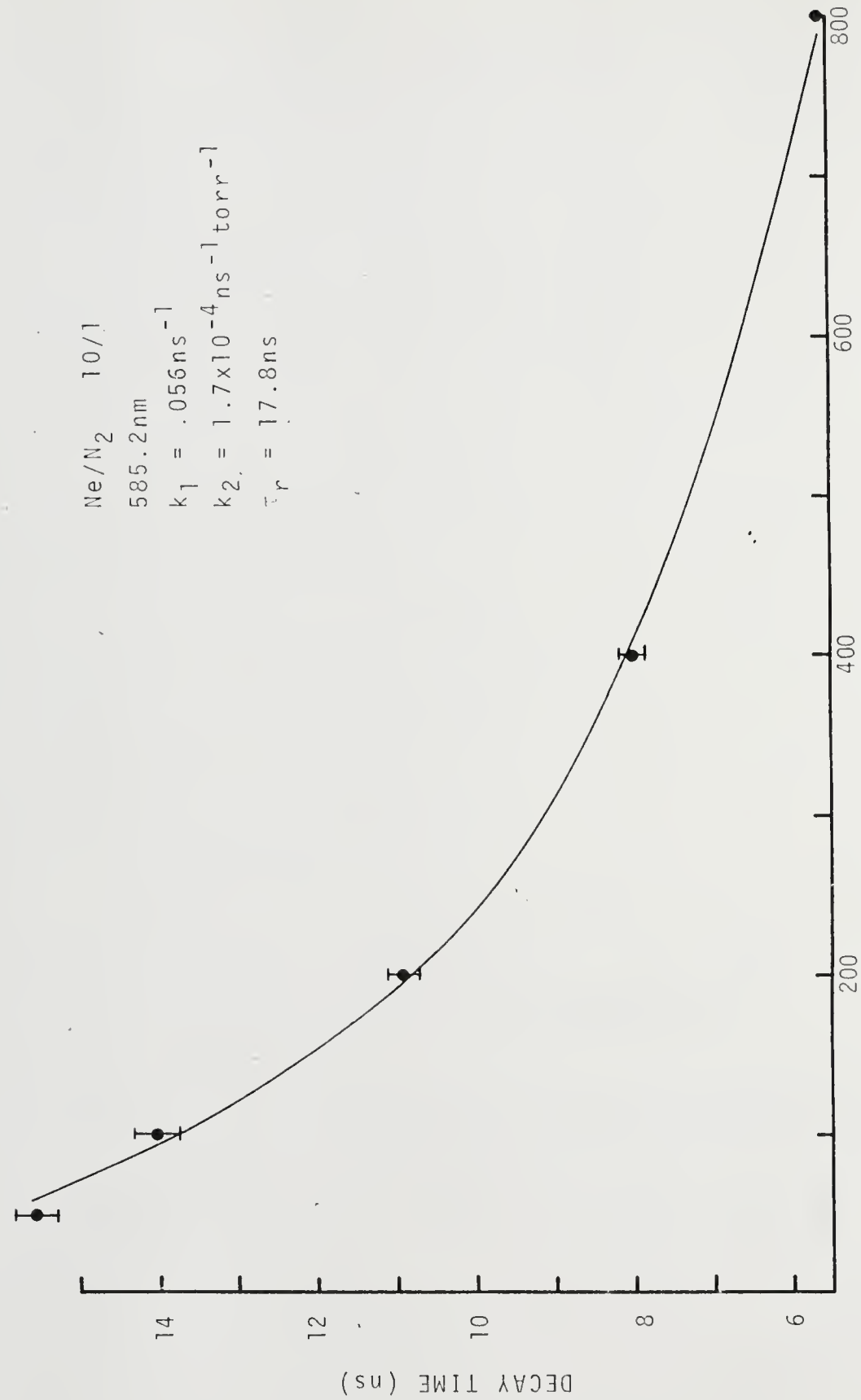

Figure 20. Decay Time Versus Pressure for 585.2nm

Figure 21. Decay Time Versus Pressure for 585.2nm

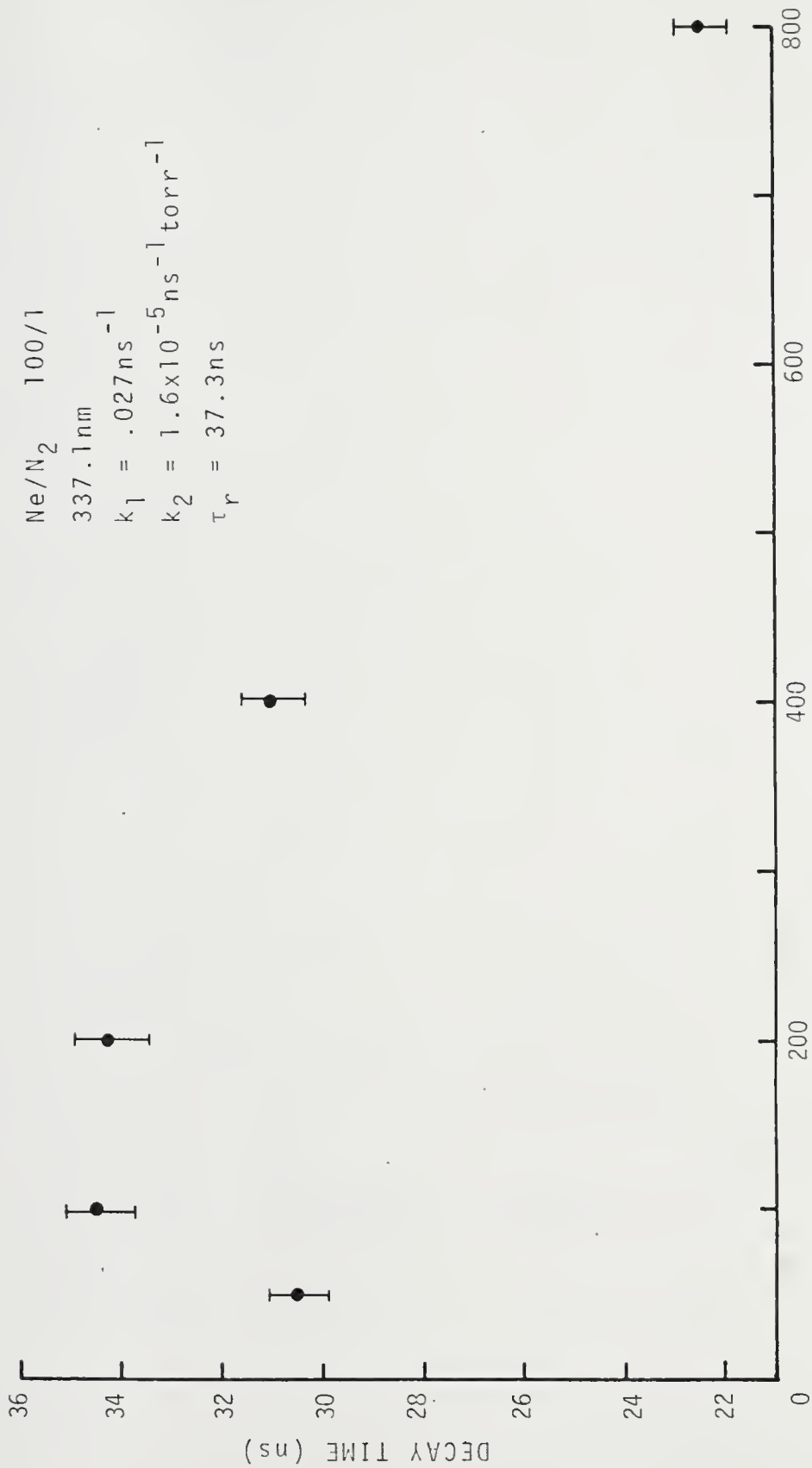

Figure 22. Decay Time Versus Pressure for 337.1nm

Figure 23. Decay Time Versus Pressure for 337.1nm

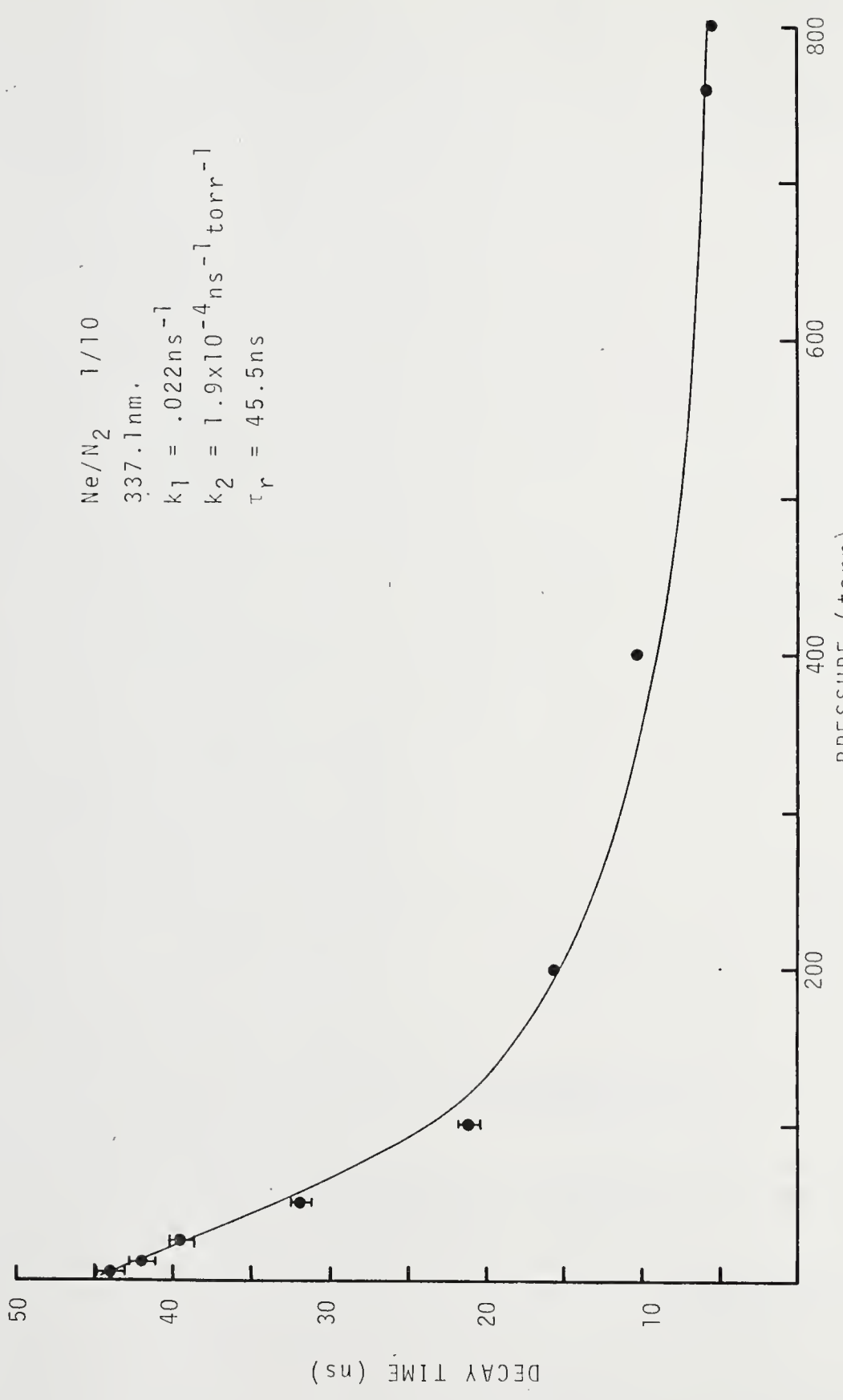

Figure 24. Decay Time Versus Pressure for 337.1nm

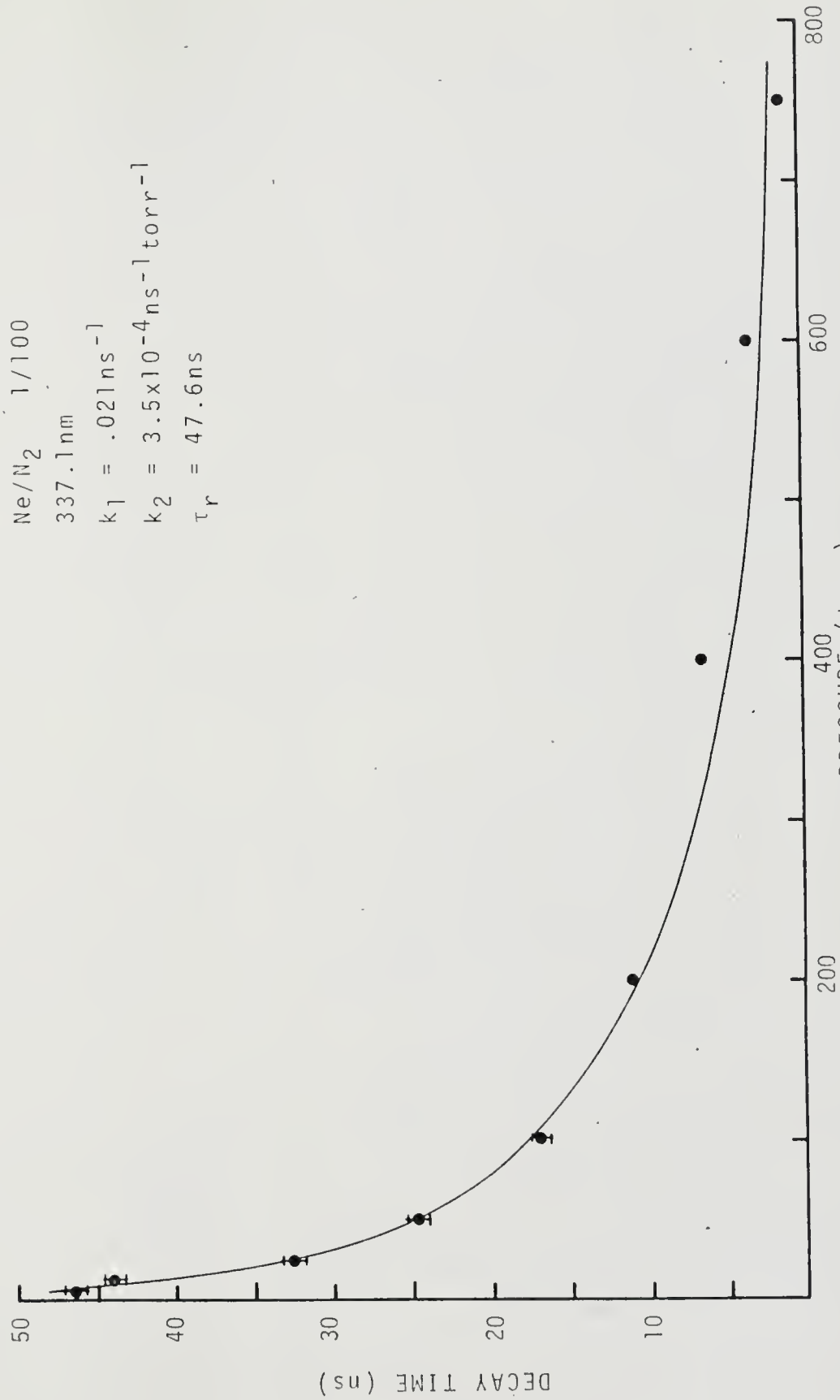

Figure 25. Decay Time Versus Pressure for 337.1nm

When we turn to the analysis of the 391.4nm and due to the N_2^+ molecular ion, which has been reported to have a radiative lifetime of about 65ns, some very strange results are observed (see Figs. 26, 27, 28). In pure neon, the first negative band due to nitrogen impurities within the gas had a lifetime of 90,000±3500ns. As the nitrogen concentrations increased to 10% and 50%, the lifetime dropped to 10,000±400 and finally, to 3800±150ns. Anomalous excitation of N_2^+ has been seen before in laser produced air plasmas,[11] argon plasma jets,[12] radio frequency plasma torches,[13] and manganese seeded plasma jets,[14] but has received no adequate explanation.

5.3 Helium/Nitrogen Mixtures

Next, let us consider helium-nitrogen mixtures. For pure helium, the emission was dominated, just as in the case of electrical excitation, by the first negative bands due to the N_2^+ molecular ion (see Fig. 29). As the nitrogen concentration increased to 1% (Fig. 30), the dominant band became the second positive system, but the first negative was still visible. This behavior is to be compared with the case of electrical excitation in glow discharge where the 391.4 emission dominated to much higher concentrations of N_2. The persistence of the N_2^+ emission may be due to the electric field inhibiting recombination and, hence, keeping the population of N_2^+ elevated with respect to the fission fragment excited case. The intensity variation of 391.4nm with pressure for several mix ratios is shown in Figure 31.

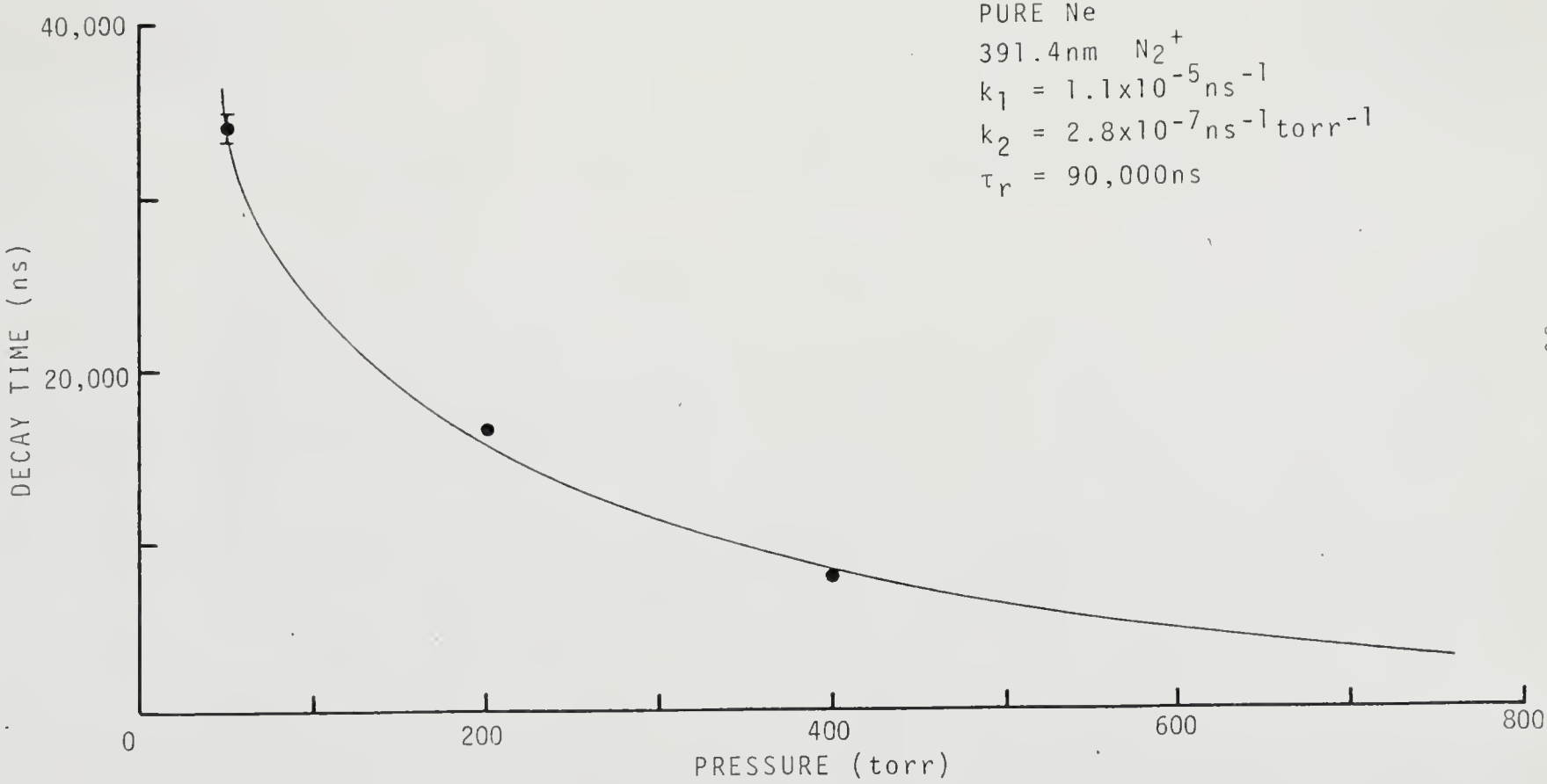

Figure 26. Decay Time Versus Pressure for 391.4

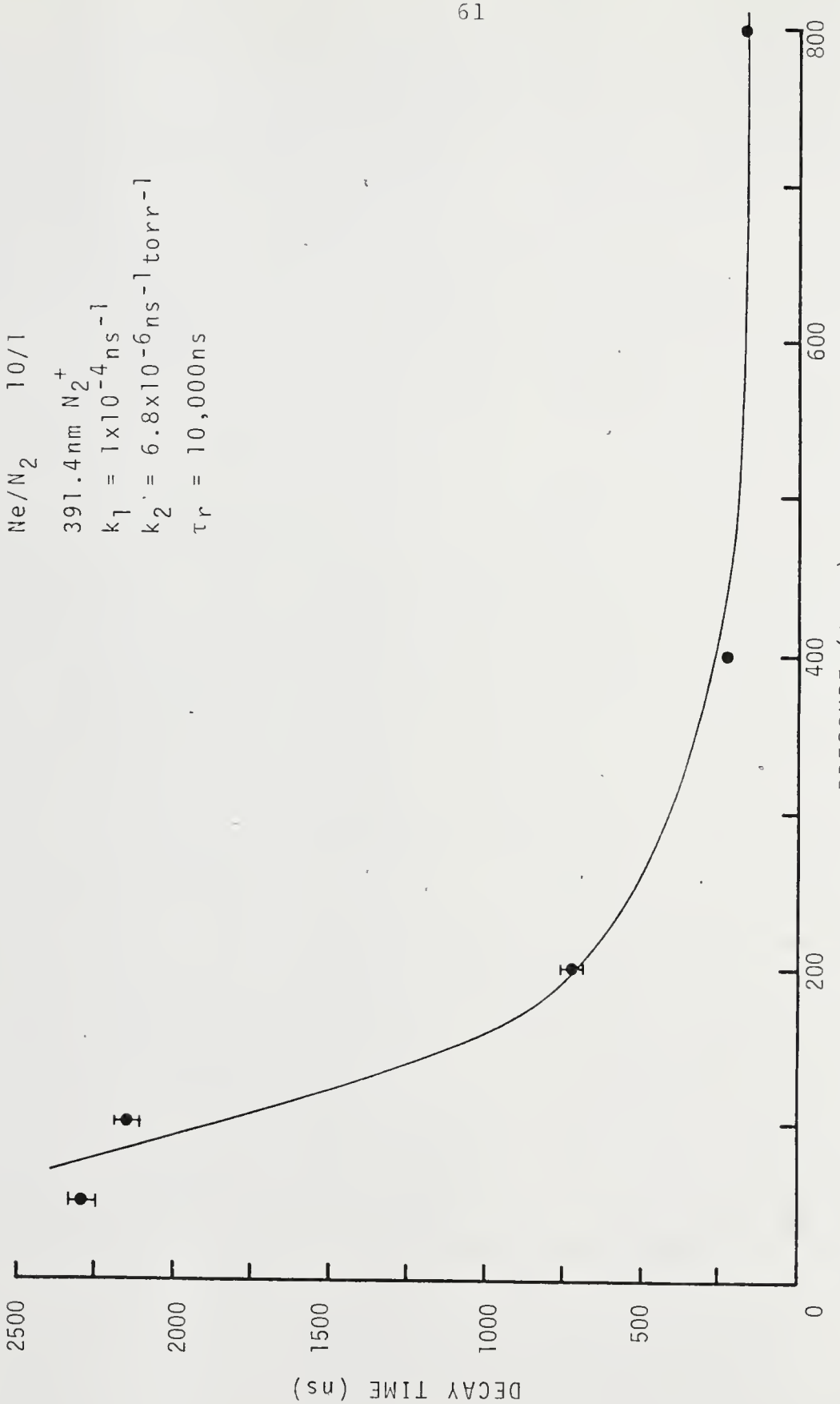

Figure 27. Decay Time Versus Pressure for 391.4nm

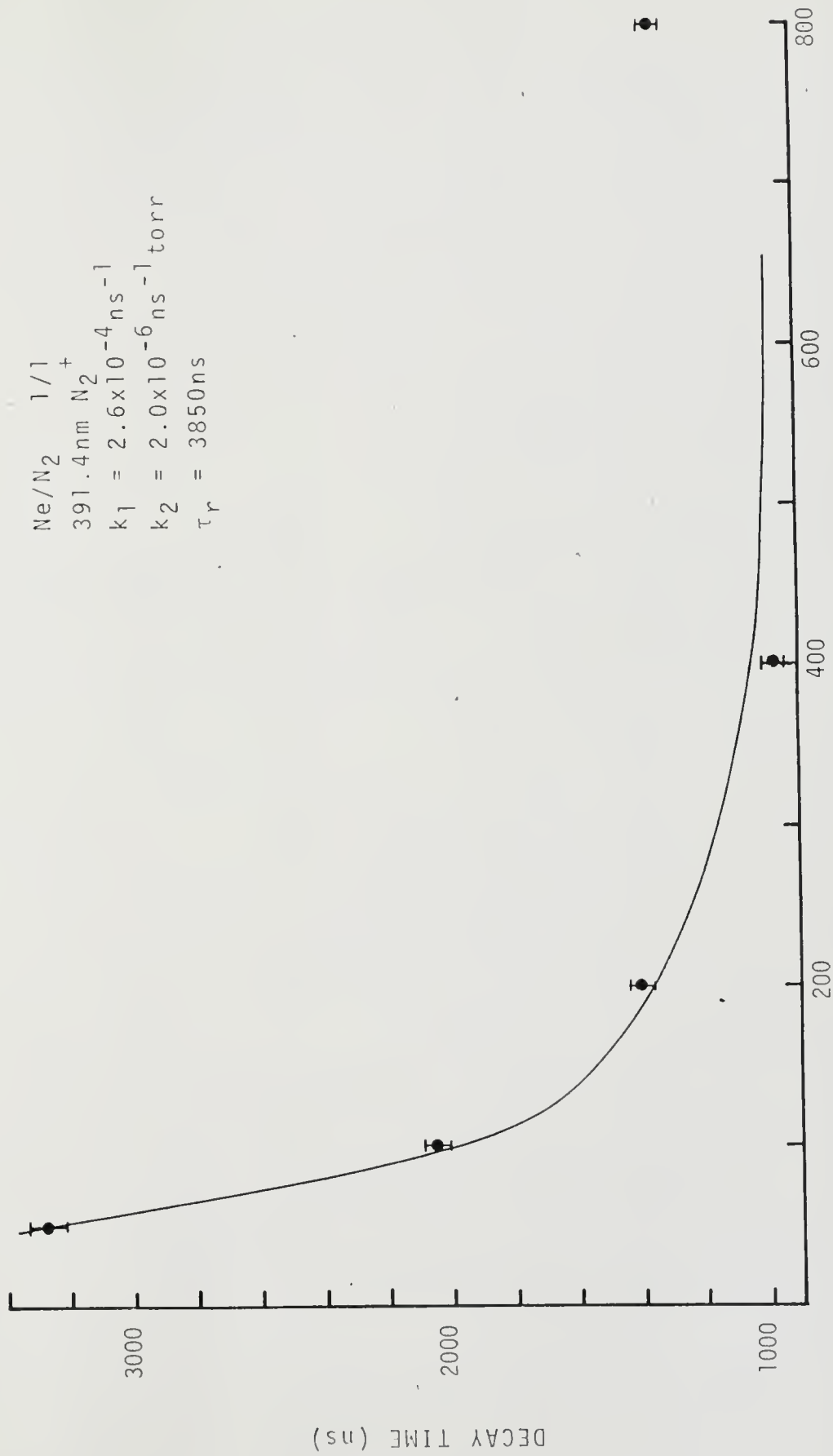

Figure 28. Decay Time Versus Pressure for 391.4nm

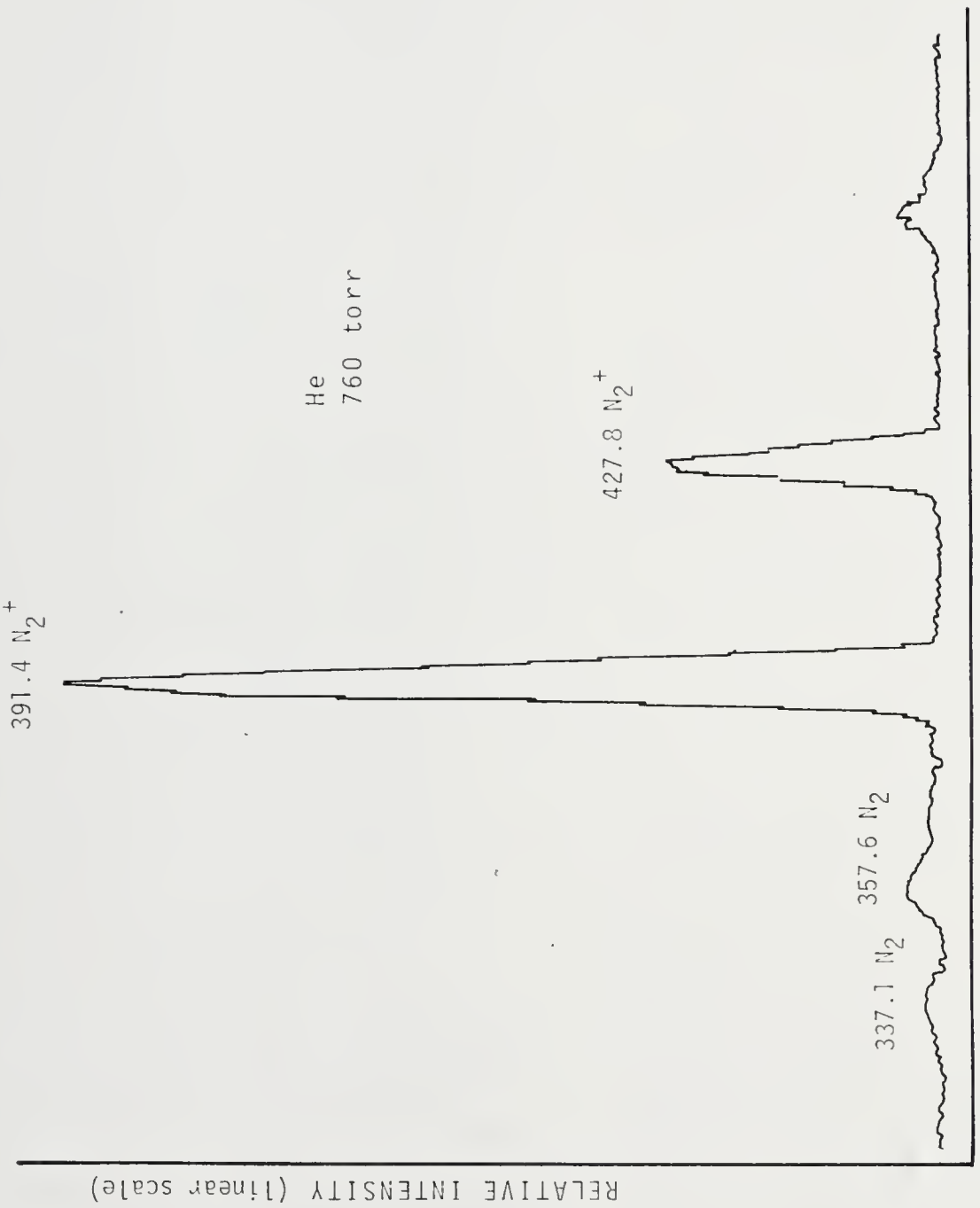

Figure 29. Scan of Nitrogen Impurity in He

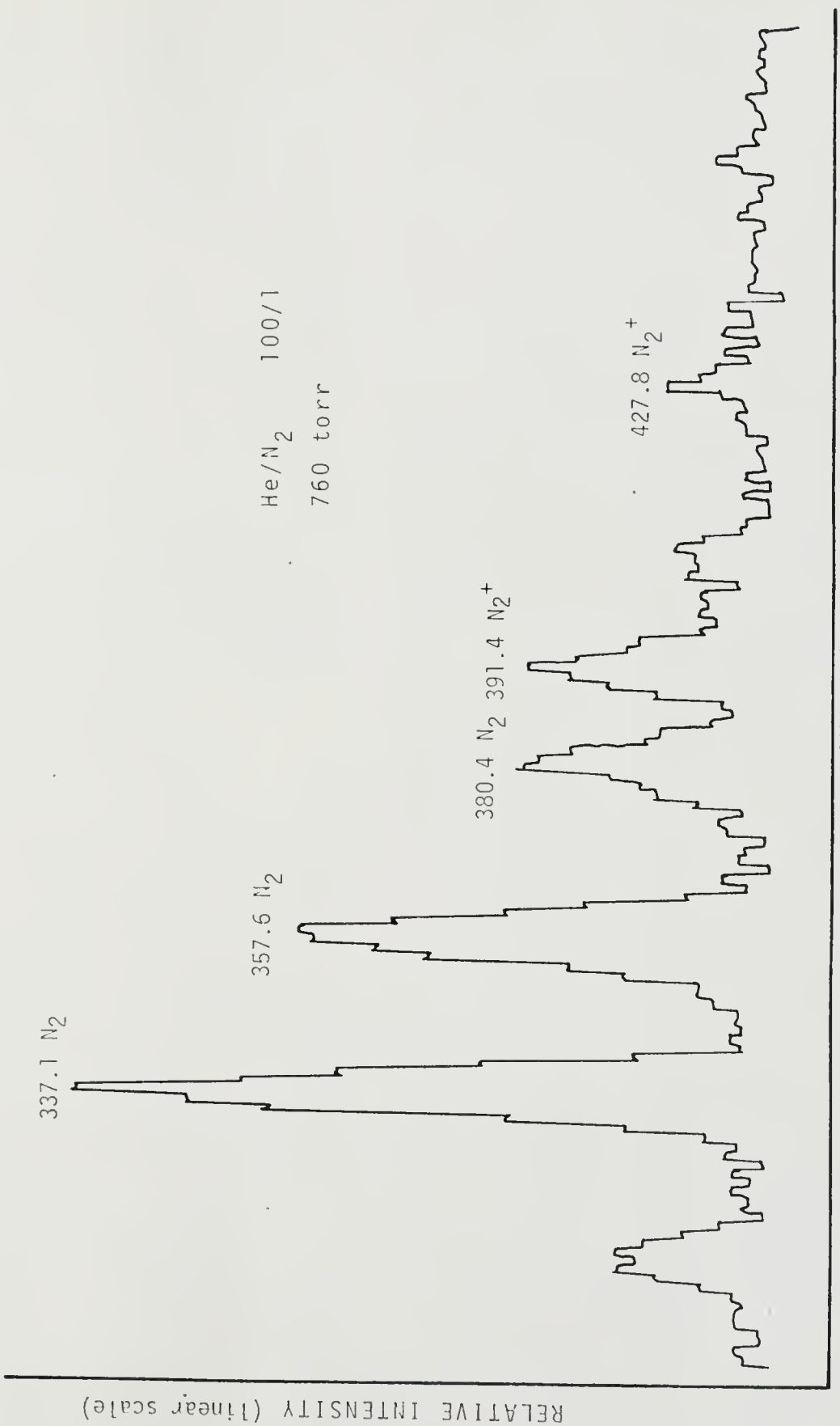

Figure 30. Scan of He with 1% N_2

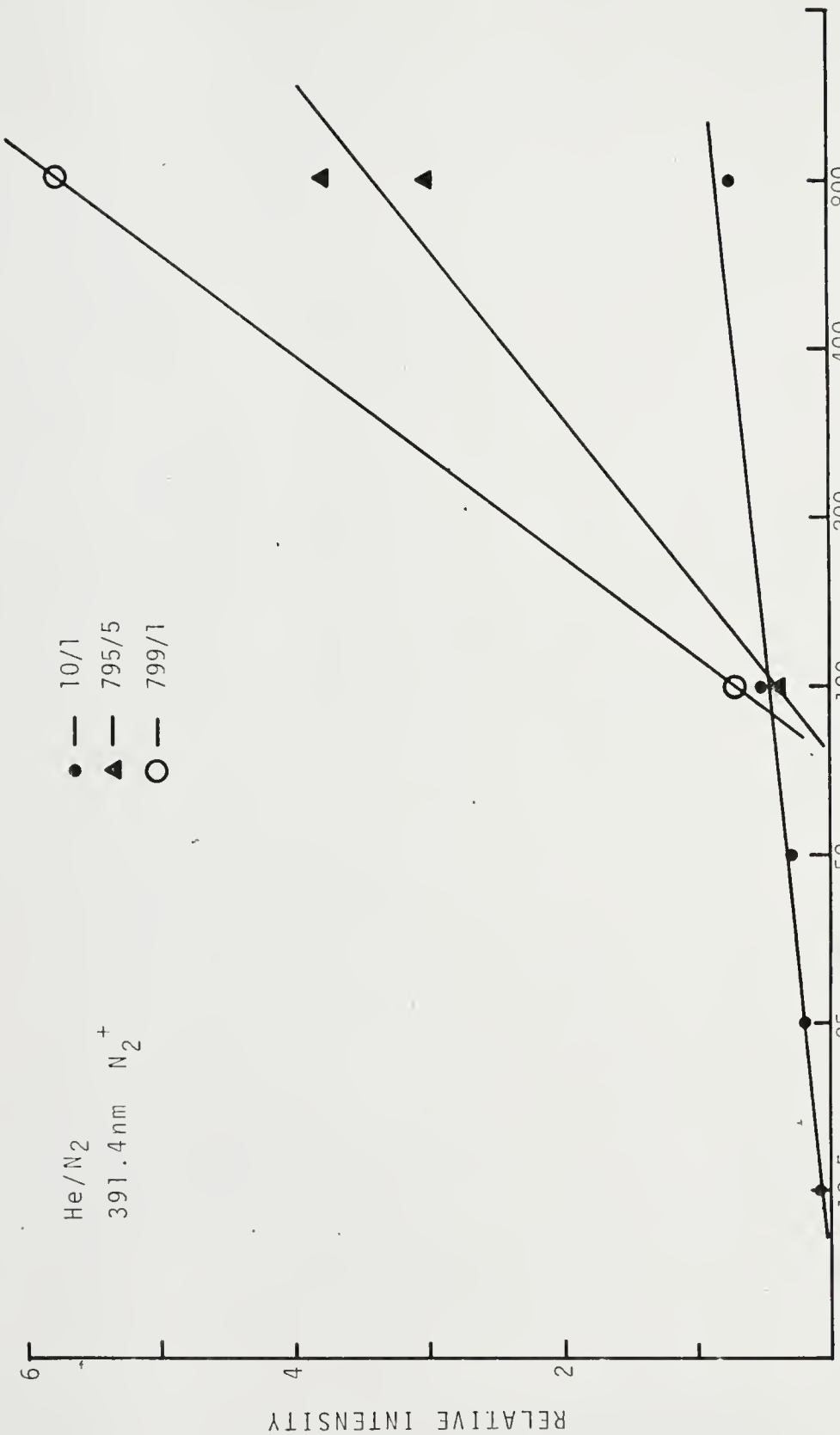

Figure 31. Relative Intensity Versus Pressure for 391.4nm

At 10% nitrogen, all observable emission was due to the neutral molecule (see Fig. 32).

Turning to the decay curve with 1/2% N_2 in helium, we see that the difference between 800 torr and 100 torr was dramatic (see Fig. 33). There was a lot more energy coming out of the gas as light, and it came out for a lot longer time even though the energy deposited by the fission fragment was less for a gas that was mostly helium than for the heavier nitrogen. Figure 34 shows the change with pressure of the decay time for various mix ratios. As the amount of N_2 decreased, the lifetimes of the N_2^+ level was increasingly determined by the helium metastable lifetime. As the amount of nitrogen increased, recombination took place much more rapidly, causing an additional depletion of the level.

Figure 35 shows a scan where the system had been adjusted to respond only to photons which were emitted during the first four nanoseconds after fission, while the fission fragment was still within the field of view, and excitation was still taking place. There appears to be no difference between this curve and Figure 29, which is from photons emitted at any time after fission.

5.4 Argon/Nitrogen

Because of the intense emission observed in the past from fission fragment excited mixtures of argon and nitrogen,[1] [2] [15] and also, because of the interest in using argon as a cover gas in the gaseous core reactor, preliminary

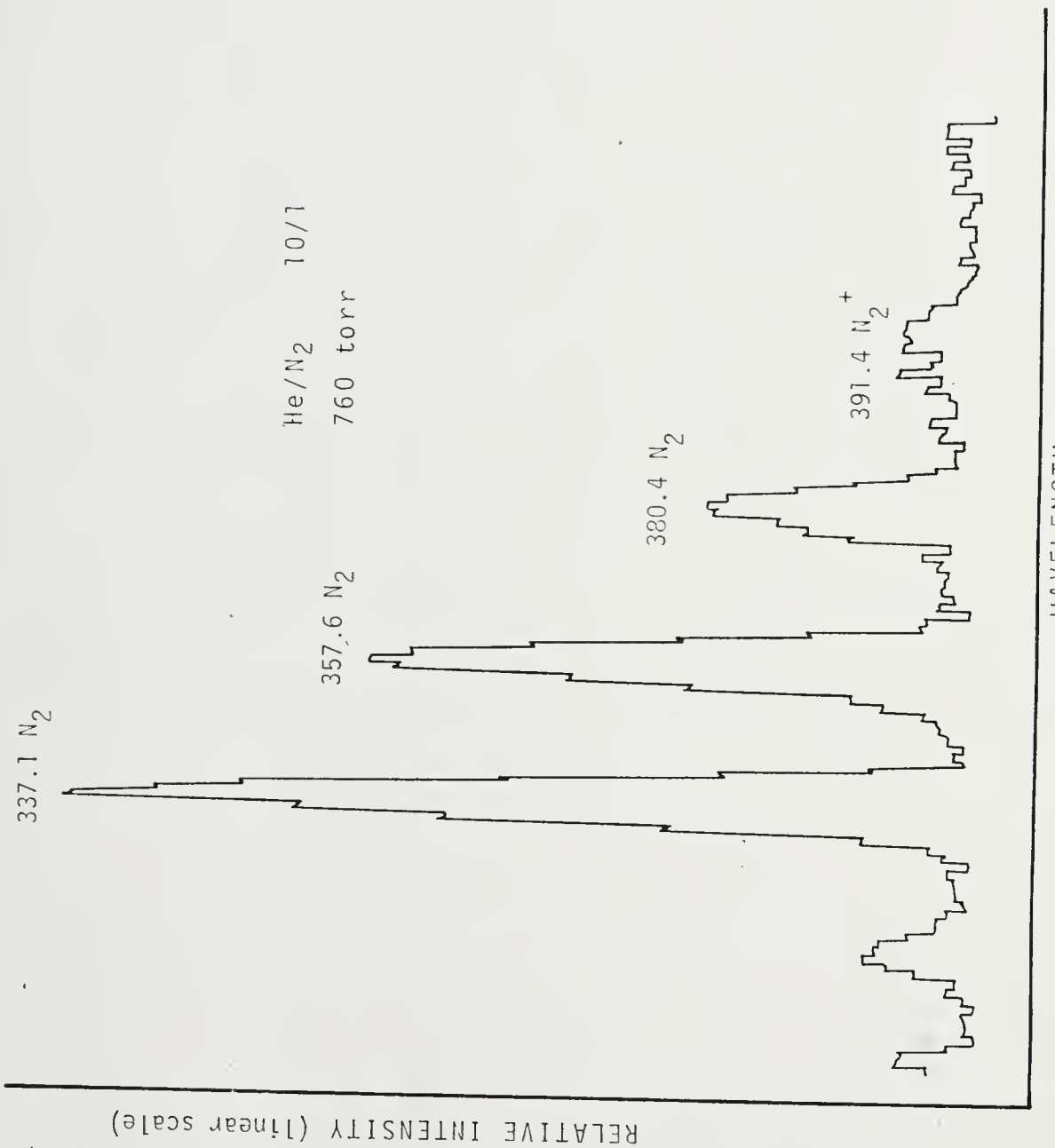

Figure 32. Scan of He with 10% N_2

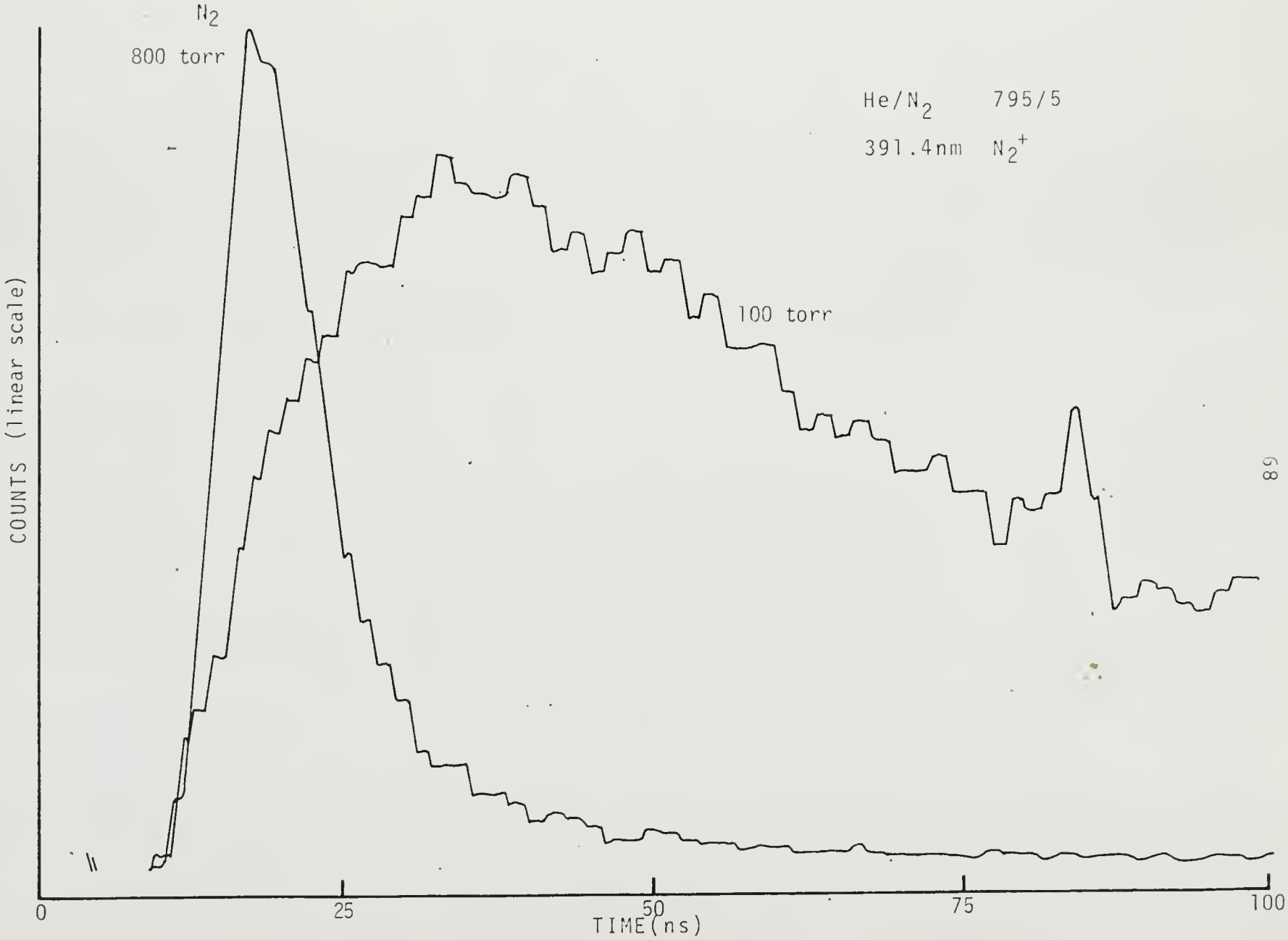

Figure 33. Metastable Transfer in He/N_2

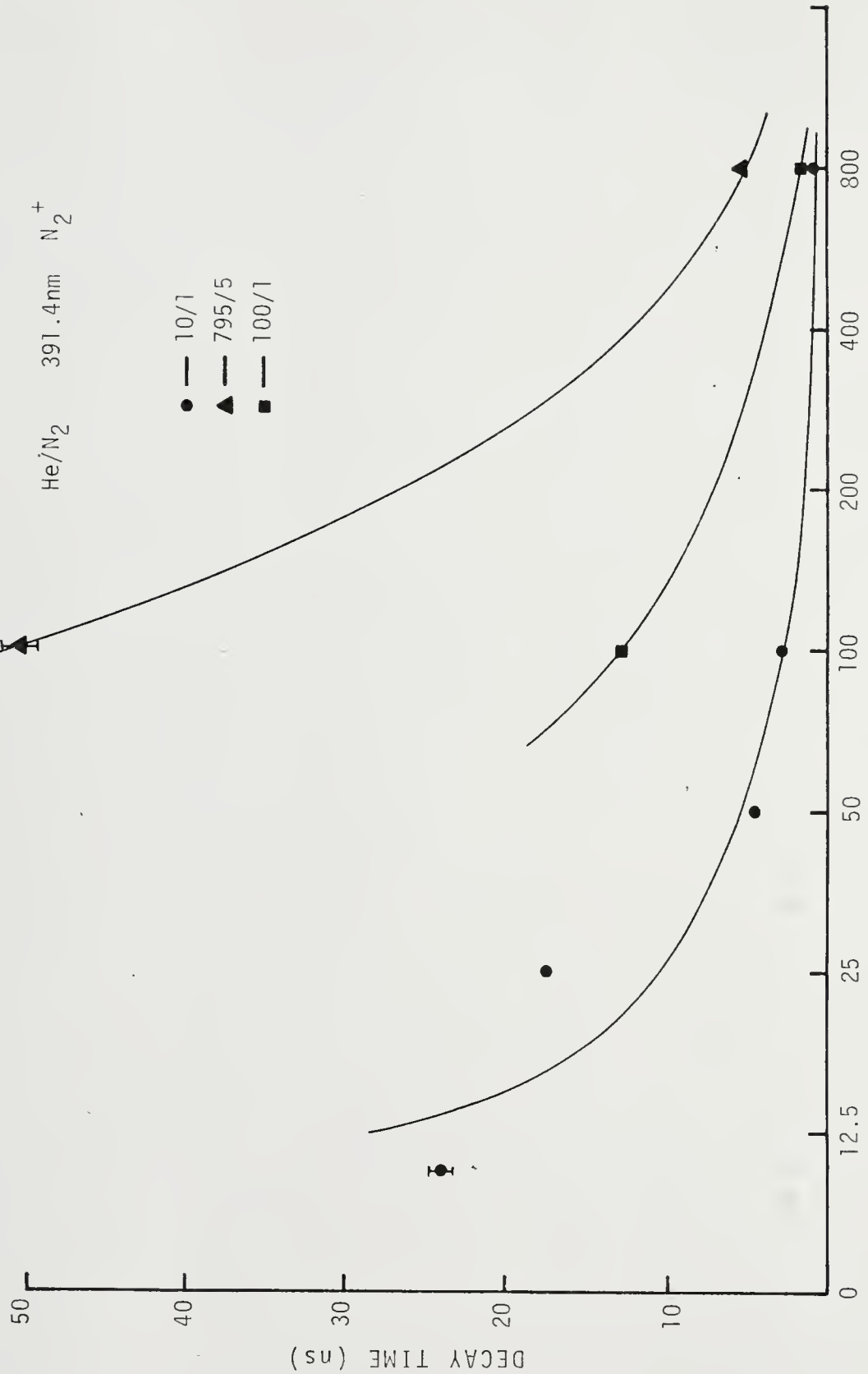

Figure 34. Decay Time Versus Pressure for 391.4nm

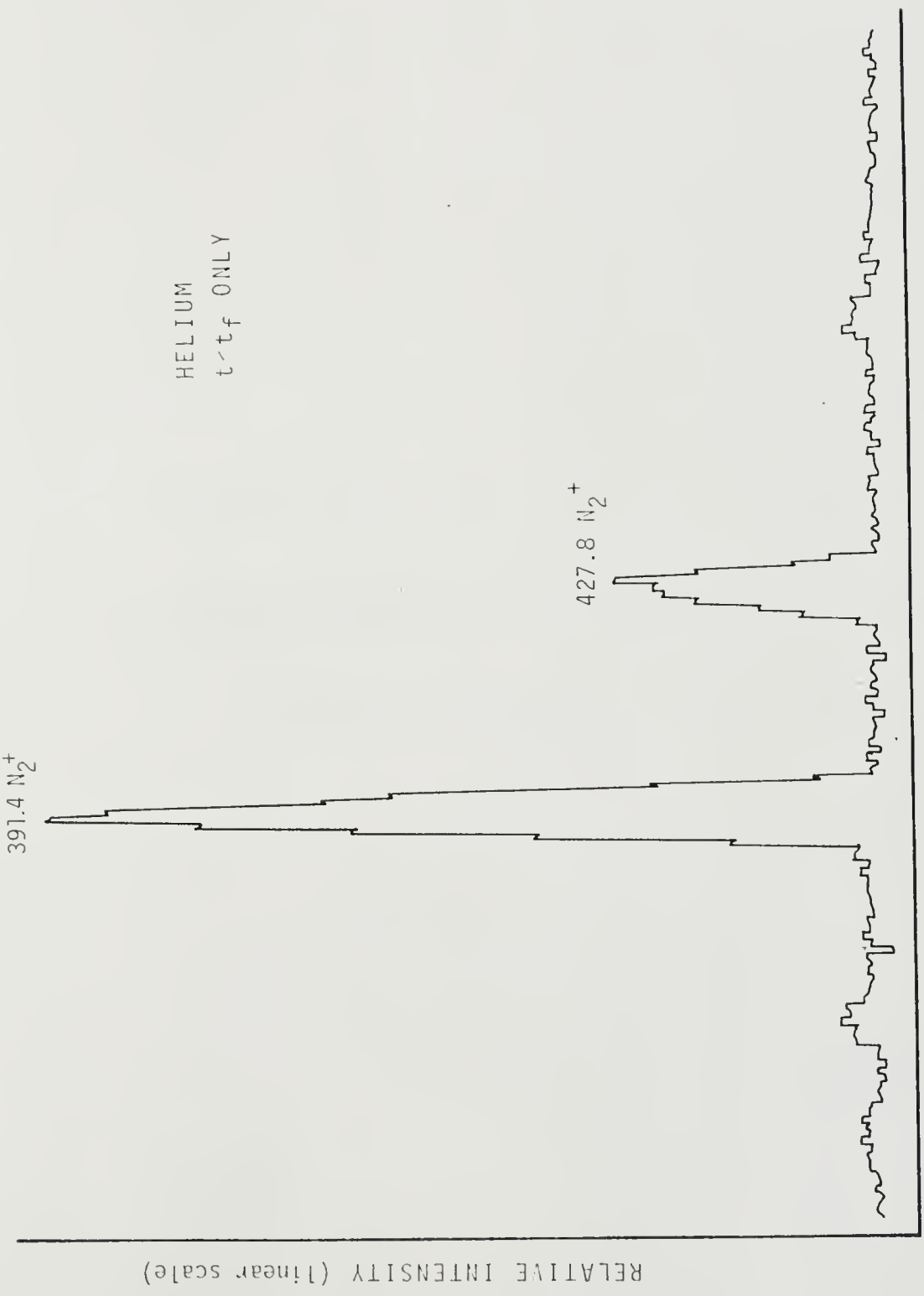

Figure 35. Scan of N_2 Impurity in He, Excitation Period Only

measurements were carried out on a 10 to 1 mixture of argon to nitrogen, the mixture that had been found previously to give the most light. Figures 36 and 37 show a spectral scan of the second positive band of N_2 which dominated the visible emission. There was very little emission in the first negative band.

Looking at the decay curves of the $C^3\Pi u$ level, we find a very instructive result. The decay curves show two components, a fast and a slow one (see Fig. 38). Quantitatively, the fast decay approaches 45 ns, the radiative lifetime of the $C^3\Pi u$ level, while the slow decay shows a zero pressure value of 600 ns. What we are observing is the fast initial decay of the directly excited nitrogen level and the slower metastable transfer from the argon 4'P level which is in resonance with it. As the pressure drops, the collision frequency decreases, and metastable transfer is no longer so important vis a vis direct excitation.

5.5 Carbon Tetraflouride

One of the peripheral interests in the optical emission of fission fragment excited gases had been the possibility of using a gaseous scintillator as an in-core monitor of the power level in the LMFBR. Early studies by Pagano[16] indicated that the fluorocarbon CF_4 had the dual advantage of being inert and having high luminosity. Pagano was not able to determine whether CF_4 or some dissociation product was causing the intense emission which he observed. Because of the difficulty of obtaining CF_4 (or Freon-14),

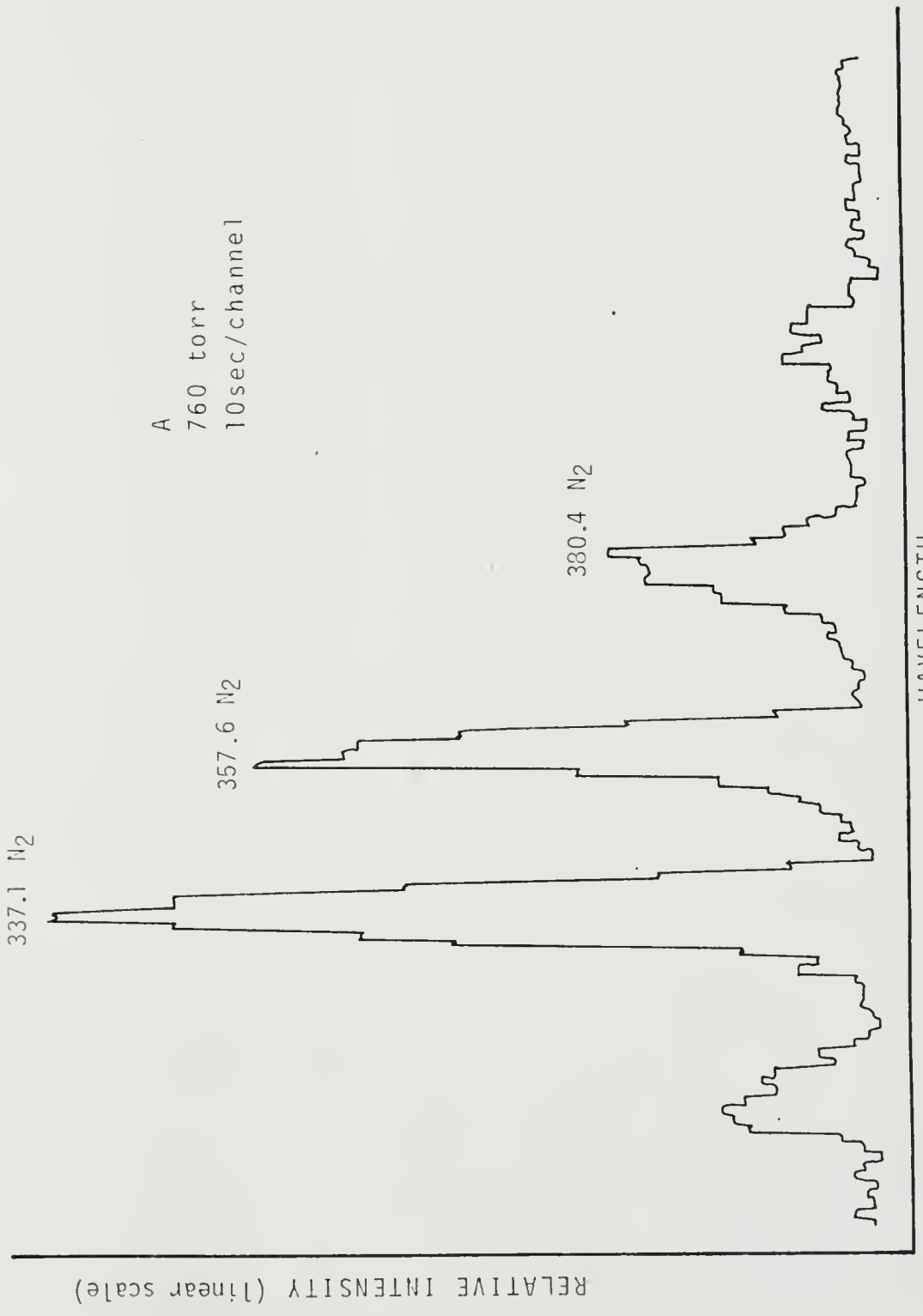

Figure 36. Scan of Nitrogen Impurity in Pure Argon

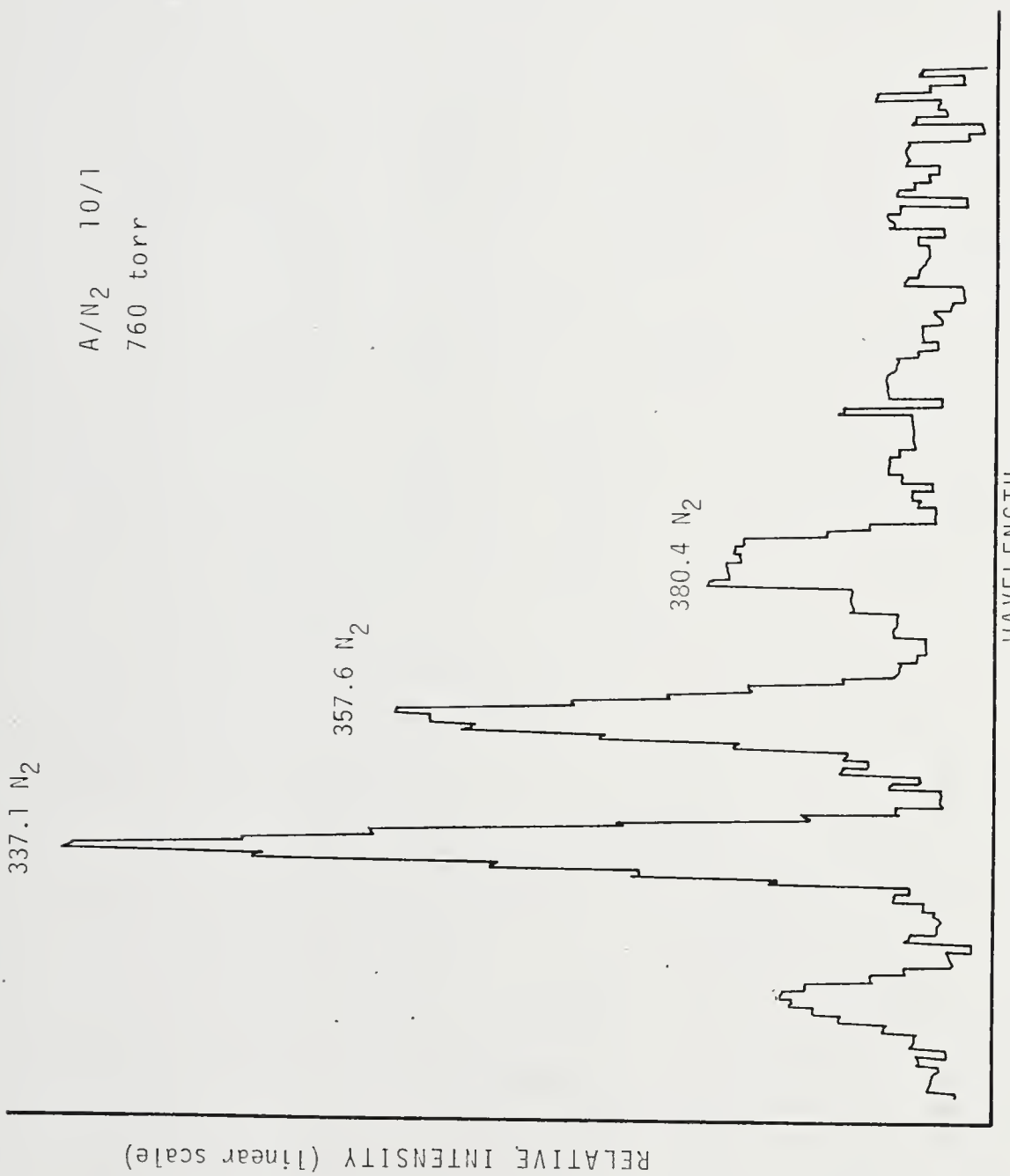

Figure 37. Scan of Argon with 10% N_2

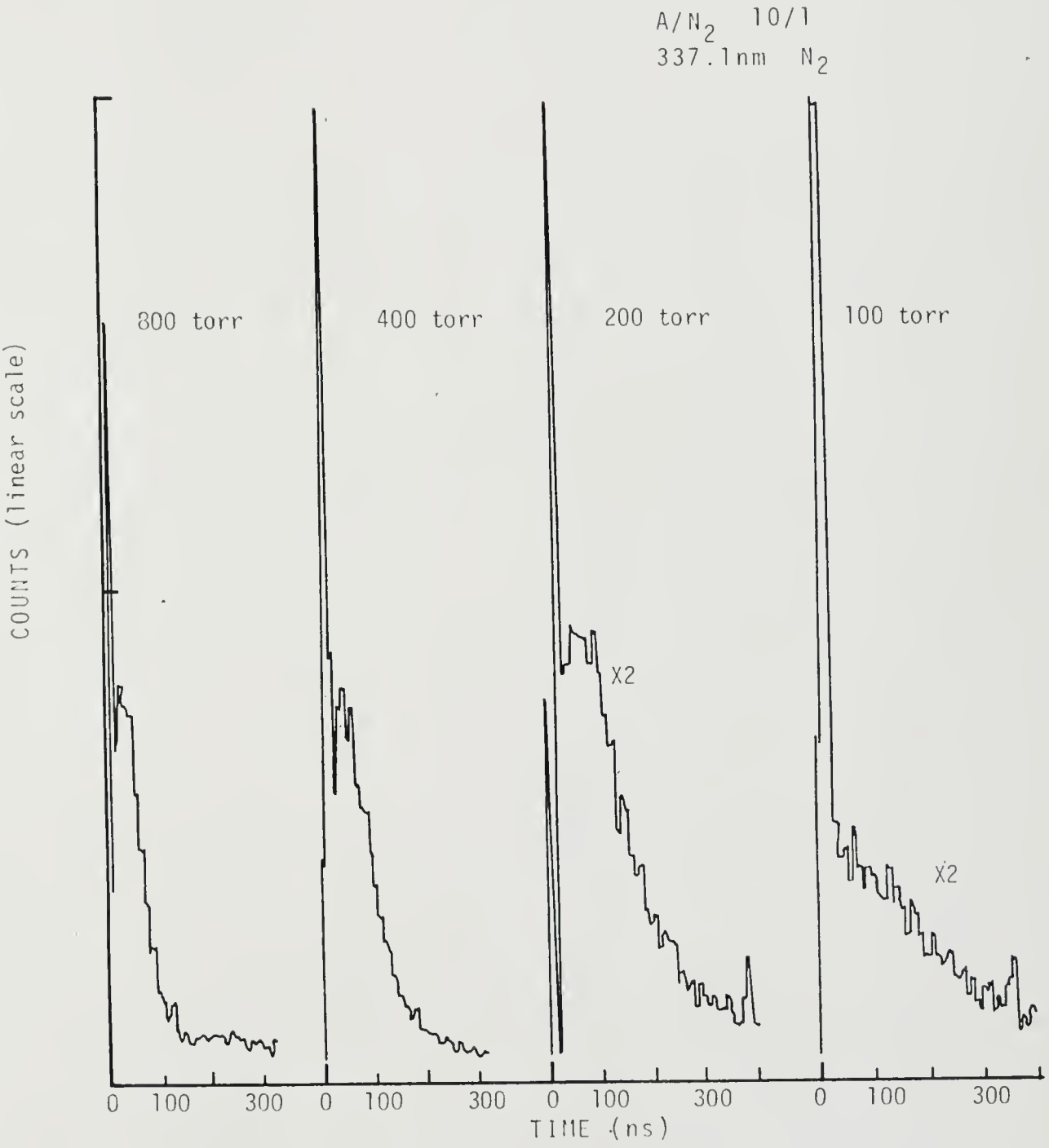

Figure 38. Fast and Slow Decay in A/N_2

only a few measurements were carried out. Spectral scans showed a broad continuum in the ultraviolet which had been previously observed by Walters.[1] A decay curve was made of the $C^3\Pi u$ level of the nitrogen impurity at 586 torr, and the decay was a simple exponential with a 1/e time of 26.2 1.0ns (see Fig. 39). This emission was much too weak to account for the intense total luminosity emission.

CF_4 was the only gas in which the present system was able to resolve the couble humped fission fragment distribution (see Fig. 15). This is thought to be due to the large amount of light given out for each fission fragment allowing much better energy resolution.

Just why CF_4 should have such a high specific scintillator efficiency is not clear, nor is it known what is responsible for the emission in the ultraviolet.

We expect the excited states of the molecule to be rather high due to the tight bonding of fluorine. The higher the initial excited state is, the greater the probability usually is of non-radiative deexcitation.[6] Dissociation following excitation has been suggested as the reason for the almost total lack of luminescence in other inorganic polyatomic molecules.[17] The same reason has been given for the absence of luminescence in saturated hydrocarbons.[18] This reason may account for the observed lack of luminosity on the part of UF_6.[19] The emission from CF_4 remains a mystery.

In all these measurements it was necessary to remember

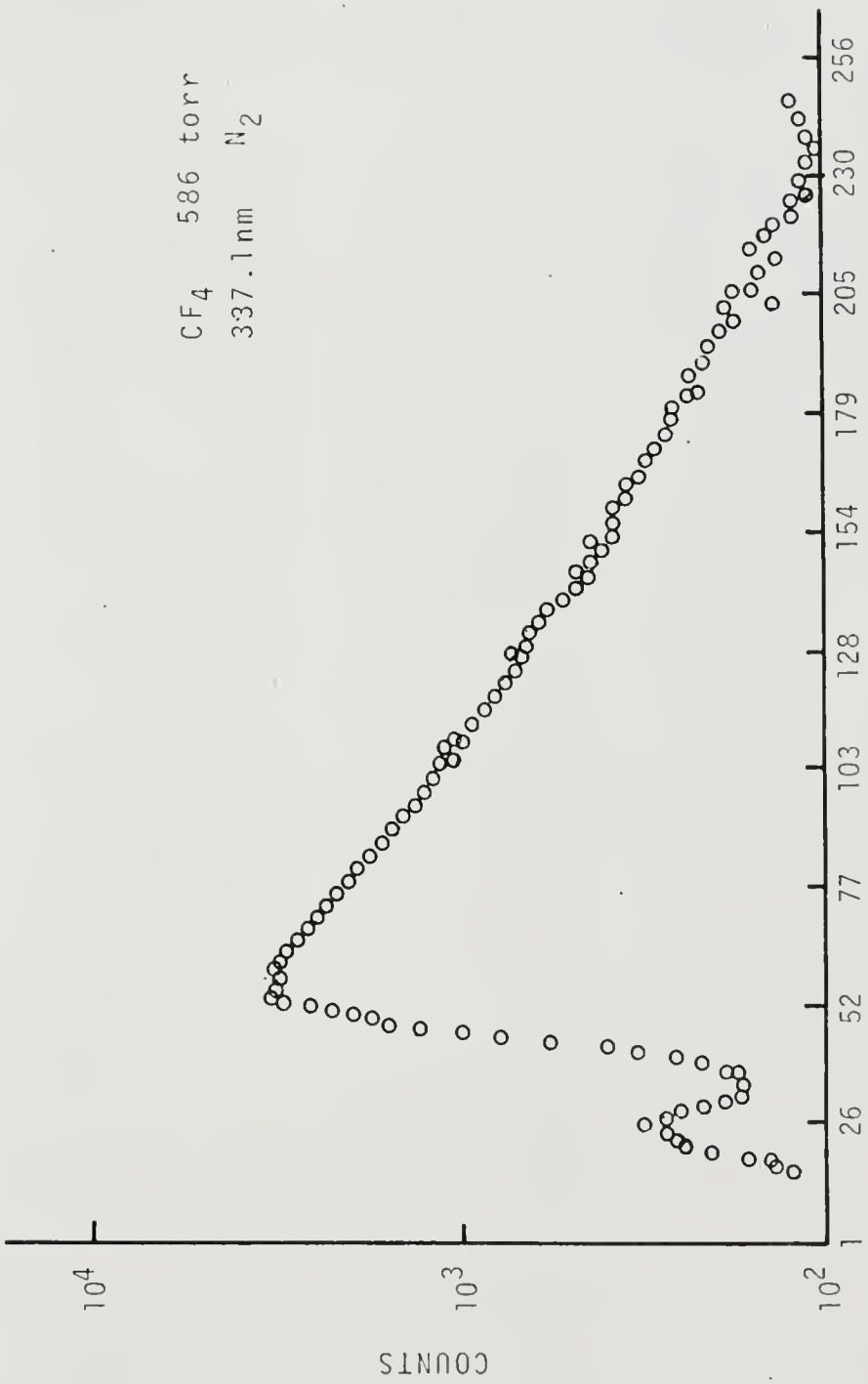

Figure 39. N_2 Impurity in CF_4

that the number of excited states and, thus, the intensity caused by the passage of a fission fragment would depend upon which fission fragment was observed. The initial energy of fission fragments varies and so does the energy deposition. If we set the discriminator level so as to trigger on only the most energetic half of the fission fragment distribution, we found as expected, that the intensity per fission fragment increased. Thus, all the measurements described in this dissertation are for the mean of all particles, and the discriminator had been carefully set to include all the fission fragments but to exclude all the alpha particles. It should be noted that in a reactor experiment, the observed emission comes from both the fission fragments and the alphas, as there is no way to distinguish excited states caused by the one from the other. Some differences may, therefore, be expected in experiments done in the two environments.

5.6 Population Inversion Study

To determine if a population inversion exists between two levels, it is sufficient to monitor the relative spontaneous emission coming from each level when, by correcting for the relative transition probabilities, we can determine the population ratio. Observation of the steady state excitation does not always reveal the presence of pulsed inversions since a long uninverted tail may mask an inversion which occurred early in time.

The most difficult problem associated with this type of measurement was finding an allowed transition whose

upper and lower levels were both within the purview of the system. Usually, if one of the transitions was in the visible, the other was in either the ultraviolet or the infrared. The laser candidate which we studied was the second positive band of nitrogen (see Fig. 8). Pulsed laser emission had been observed previously,[20] and so this band provided a good choice for testing the method. In addition, we had available a computer solution of the rate equations of nitrogen (Fig. 40) for electron beam excitation.[21] These solutions were of the form I versus t, exactly the output of the system. The upper and lower levels of this band system are the $C^3\Pi u$ levels which could be monitored through the second positive emission itself, and the $B^3\Pi u$ level which gives rise to the first positive group (Fig. 41). The measured populations and the way they changed with time had the same form as that predicted by the solution of the rate equations and showed the same decay rate when allowance had been made for the difference in pressure between the computer solution (3 atmospheres) and the experiment (1 atmosphere).

Figure 40. Population Densities of $N_2(B)$ and $N_2(C)$ Versus Time

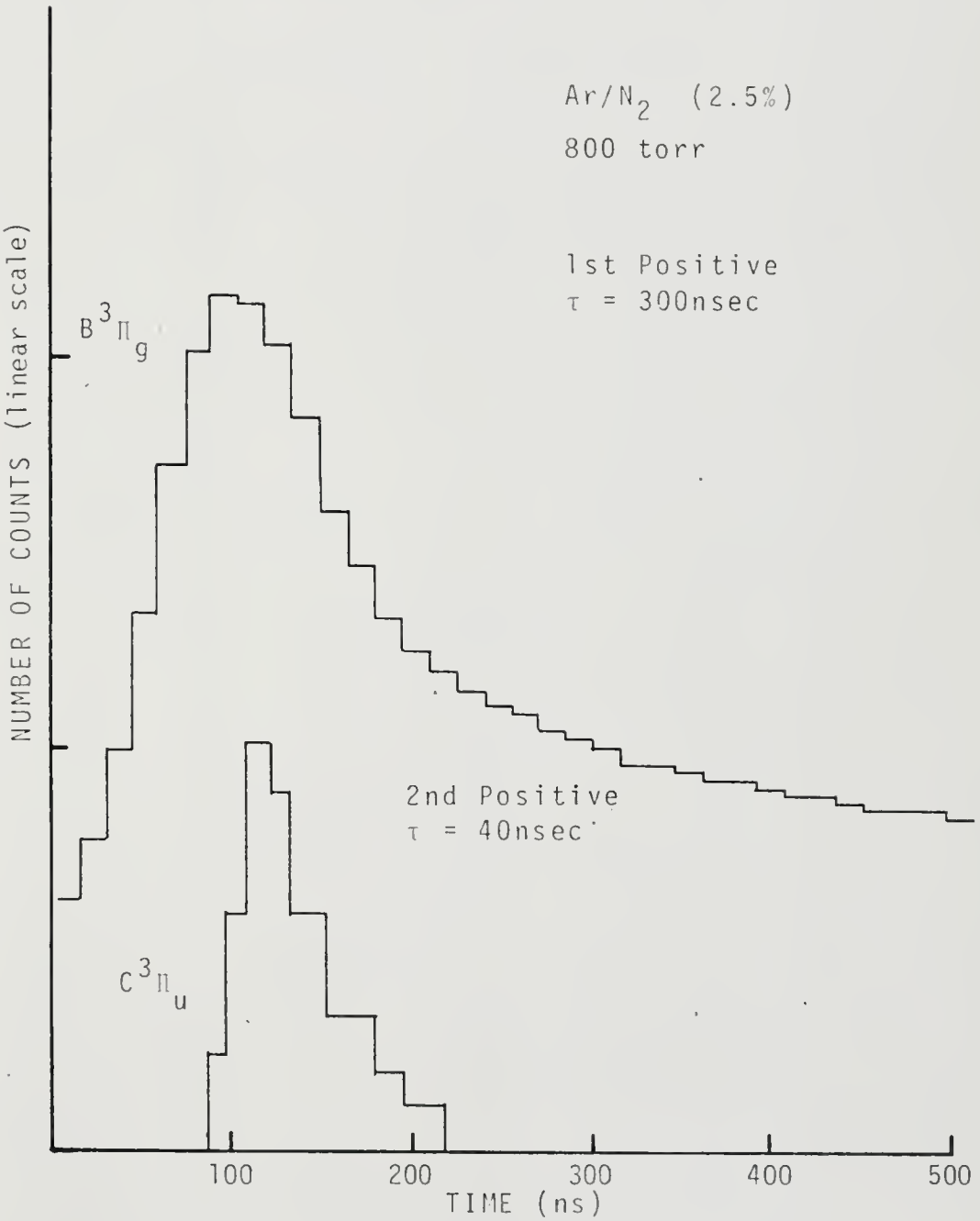

Figure 41. Measured 1st and 2nd Positive Populations

CHAPTER 6

CONCLUSIONS AND FUTURE WORK

6.1 Conclusions

The conclusions arrived at in this research fall naturally into three categories: conclusions about the system, conclusions about pure nitrogen, and conclusions about gas mixtures and fission fragment excited gases in general.

The detection system was similar to existing fluoresence decay systems except that no trigger pulse was necessary, and so sources that were non-periodic, transient, and randomly occurring could be studied. The system was extremely sensitive, capable of counting single photons, and was relatively insensitive to gamma background. The source, unlike a discharge, did not cause extensive thermal decomposition or dissociation of the test gas, nor was it necessary, as with a flash lamp, that the level of interest be connected to the ground state by an allowed transition. The system could measure times as short as 1.7ns and, perhaps, shorter. It had repeatability of better than 4% and a minimum resolving time of about 1ns. The minimum resolving time was limited by the photomultipliers and could be improved as photomultiplier transit spread is improved.

The results obtained for the $C^3\Pi u$ level of pure

nitrogen were the same within experimental error as those obtained by others in the past (see Table 1). The gas had a single decay time and showed no deviation from two-body quenching until 800 torr. There appeared to be no other source of excitation to this level other than by the secondary electrons. The energy deposition by the fission fragment was found to exhibit an almost perfect square law dependence and is a maximum when $t_f = \tau/Z^2$.

Comparing Figures 11 and 13, we may observe that a pulsed laser might operate best at a differenct pressure than would a CW laser. Since, in the pulse case, we are interested in the greatest instantaneous population, we would choose the peak in Figure 11, while for the steady state case, we are concerned with the average population density and would follow curve 13.

Looking at other gases and gas mixtures, we found that CF_4 gave the greatest light output with a 10/1 argon/nitrogen mixture second. For the mixture neon/nitrogen, where there are no resonant interactions, whatever level was being observed showed only small changes from the pure gas case except that the decay time was determined by the total pressure and not the partial pressure of the observed gas. The lifetime of the N_2^+ molecular ion showed extremely large values when nitrogen was a small impurity (less than 1%). No explanation for this behavior was found. In argon/nitrogen and helium/nitrogen, the lifetimes were dominated by resonant collisions with metastables. In argon,

TABLE 1

Lifetime (nsec)	$k_2/k_1 \times 10^2$ *(torr^{-1})*
40.5±1.3	1.75±0.06
48.0±8.0	1.60±0.16
46.3±1.0	1.70±0.20
49.0±5.0	---
37.0±3.0	1.49±0.04
38.2±8.0	---
35.5±2.0	1.50±0.20
48.0	1.67±0.29
44.5±6.0	---

Previously Published Values for $C^3\Pi u$

Reference No. 5

the $C^3\Pi u$ showed some enhancement while in helium, the $B^2\Sigma u^+$ was tremendously increased.

6.2 Future Work

Much work remains to be done using the isotope excited fluoresence decay system to further characterize fission fragment excited plasmas. The inclusion of an electric field within the experimental chamber would allow the separation of effects due to ions from those due to neutrals. In addition, the electric field could be used to increase the light output, thus, reducing the demands on the spectroscopic apparatus. Cooling the chamber would allow the study of gases which undergo thermal decomposition at room temperature.

In order to separate the effects of the fission fragments from those of the secondary electrons, a beta source (such as ^{12}C) might be included in the chamber. The beta energy distribution spectrum of ^{12}C closely resembles that of the secondary electrons created in fission fragment bombardment. A shutter over the fission fragment source would allow observations to be made of the gas with electron excitation alone or with fission fragment plus electron excitation.

Another use of this system is for studying extremely electronegative gases. These gases, of which UF_6 is one of particular interest, are difficult to excite using electrical charges, and one must often resort to "seeding" an inert gas with small fractions of such molecules.

Still another use of this system is in the serach for possible fission fragment excited laser inversions. Since

the system provides time resolution, it is possible to identify inversions which are quenched at long time and are, thus, candidates for pulsed operation.

This system would also work well for studying liquids.

6.3 Scanning Mode Recommendations

A major improvement in the scanning technique could be experienced through the use of a minicomputer or microprocessor. The scanning rate could be controlled in such a way that when there was no signal (as determined by comparing the count rate against background), the system would be stepped quickly. When a spectral feature is reached, the system would step slowly enough to achieve any required level of statistical accuracy.

Another interesting system could be developed to combine the features of the scanning system and the fluorescence decay system. In this mode, the system would accumulate a decay curve, read it out, step to a new wavelength, and repeat the process. This mode would be of use where there is emission continuum such as the xenon excimer band where the lifetime varies across the band. A scan of this nature would allow one to choose the region best suited to lasing.

APPENDIX 1

ENERGY DEPOSITION

The whole question of how many excited states are produced by a fission fragment revolves about the exact form of the energy deposition equation.

The Bohr energy loss equation describes the slowing down of a fission fragment due to electron collisions as

$$\frac{dE}{dr} = \frac{4\pi N(Z_{eff})^2 e^4 Z_N}{M_e V^2} L_e,$$

where e = electronic charge,

Z_{eff} = effective charge of fission fragment with velocity V traversing a medium of atomic number Z_N,

L_e = logarithmic summation term, and

V = velocity.

A semi-empirical expression for Z_{eff}, also due to Bohr, is

$$Z_{eff} = Z_{ff}^{1/3} (V/V_0),$$

where Z_{ff} = the atomic number of the fission fragment, and

V_0 = the velocity of the electron in the first Bohr orbit.

For a gas, $\frac{dE}{dr} = -kV$. Integration gives $E = E_0(1-r/R)^2$. This expression has been described as giving poor agreement with experimental data.[9] From energy loss measurements in gases, the exponent has been assigned a value from 1.5 to 1.7. Axtmann[10] has derived an expression for the intensity

of the fission fragment excited gas in terms of the exponent in the energy deposition equation. Let

$$E_d = E_0 - E = E_0(1-[1-r/R]^n) \tag{1}$$

be the energy dissipated in the gas.

A binomial expression of Equation 1 gives

$$E_d = E_0 n\beta[1-\beta(n-1)P/2]P, \tag{2}$$

where $\beta = r/R_0P_0$, and 0 refers to one atmosphere. Now the measured intensity equals

$$I = (\varepsilon Q E_d)\ F[\frac{k_1}{k_1+k_2P}], \tag{3}$$

where Q is the number of excited states formed per unit energy loss in the gas; ε is the collection efficiency; F is the number of fission fragments per second; $\frac{k_1}{k_1+k_2P}$ is the probability of light emission by an excited molecule; P is the pressure in torr; k_1 and k_2 are the radiative and collisional decay constants with units of sec^{-1} and mm^{-1} sec^{-1} respectively.

Substituting Equation 2 into Equation 3, differentiating and setting $\frac{dI}{dP}$ equal to zero gives

$$1-(1-P_m)^n-\frac{n\beta(1+\frac{k_2}{k_1}P\ )(1-\beta P_m)^{n-1}}{k_2/k_1} = 0,$$

where n is obtained implicitly in terms of β, k_2/k_1 and P_m the pressure of maximum luminosity. For this experiment $\beta = \frac{4.11}{2.2\times800} = 2.335\times10^{-3}$, and $P_m = 300$ torr. Thus,

$$1-(1-2.34\times10^{-3}\times300)^n-[\frac{n\times2.34\times10^{-3}(1+.018\times300)(1-2.34\times10^{-3}\times300)^{n-1}}{.018}] = 0$$

A fit of our experimental data gives n = 1.98 within 1%, sufficiently close to two to justify using the expression, $E = E_0(1-r/R)^2$.

APPENDIX 2

NE-111 AS A CALIBRATION SOURCE

After the delayed coincidence single photon counting system had been assembled and tested, a search was made for a fast, low level light source to calibrate the timing measurement. The characteristics required of the source were:

1) The pulse should have as small a half-width as possible and resemble in shape the fission fragment pulse.
2) The pulse amplitude should be as near that of the fission fragment pulse as possible, on the order of 10^6 photons.
3) The source should be small so that it would fit in the experimental chamber. The optimum solution would have the source small enough that it could be inserted in the chamber through one of the gas access ports so that the calibration could be done without disturbing the system.
4) The source should have near 4π geometry so that it could be observed by both photomultipliers simuntaneously.

Normally, single photon counting systems are calibrated

using a tungsten ribbon lamp and filters. This was clearly not possible in our case since we needed a pulsed source. Choppers were briefly considered, but the rotation speeds necessary to achieve chopping speeds of 1ns were considered excessive.

Fluorescence decay systems are normally calibrated using a quenched spark source. This source was too large, too bright, and too expensive to fit easily into this system.

The solution was a small chip of NE-111, a fast plastic scintillator mounted on the end of a short length of copper tubing brazed to an 1/8-inch pipe plug which could be screwed into the gas system access port. The NE-111 was secured to the end of the copper tubing by heating the tubing and pressing the plastic into the end. The length of tubing was so chosen that when the plug was screwed all the way in, the source was in the center of the field of view.

The shape of the light pulse which NE-111 emits when struck by a gamma ray is well known, having a full width at half maximum of 1.54ns and a decay time of 1.7ns. The output peaks at about 370nm, a wavelength well suited to most spectroscopic systems.

In use, the calibration source was placed in the center of the experimental chamber and viewed by the detection system. Since both photomultipliers were seeing the same light pulse, the measured time interval, corresponding to

no time difference, was subtracted from all decay measurements. This zero time interval was caused by differences in cable lengths, light paths, and photomultiplier transit times.

APPENDIX 3

GAMMA VERSUS TLP FOR START PULSE

As described in Chapter 3, a test was made to determine if using the prompt fission gammas gave the same decay curve as using the output of the TLP. Figure 42 shows a pair of measurements of the decay of the $C^3\Pi u$ state of nitrogen. In both cases, the stop pulse was supplied by the SPL while the start pulses were supplied by the TLP (the •'s) or the gamma detector (the Δ). The count was continued in each case until 512 counts had been accumulated in the peak channel. The decay times determined from the two curves are well within the 3% statistical precision of the experiment. Thus, from the standpoint of accuracy, there was no distinction between the two methods of timing; however, using the TLP provided a count rate about 1000 times greater than using the gamma detector. For this reason, all measurements were made using the TLP.

Figure 42. Using Gamma Versus TLP as Start Pulse

APPENDIX 4

GAS PURITY

One question which had to be addressed each time a run was made was "How long must the vacuum system be pumped on so that the residual impurities and the impurities which leak in and out gas off the walls during the course of the experiment will not affect the results of the measurements?"

Clearly, if the purity of the test gas was low, the system need not be pumped so long as if research grade gas were being used. As an example, assume that the test gas has a purity of 99.9995% or 5ppm impurity which sets the lower limit on gas purity. Suppose the impurity that the experimental apparatus contributes to the gas is required to be at most 10% of that figure or 0.5ppm. Then, if the chamber is filled to 240 torr pressure, the equivalent impurity pressure from the system must be no more than 240x 0.5×10^{-6} torr or 0.12 microns. However, if the count is extended one, and the impurity level is to be no greater than this at the end of the measurement, the system must be pumped farther down before admitting the test gas. It was found that when the system had been pumped to its ultimate pressure of 5×10^{-9}mmHg, it required 72 hours for the pressure to rise to 0.1 micron. Therefore, for those experiments requiring the greatest degree of gas purity, namely low

pressure ultra pure gas, the count was limited to 72 hours. On the other hand, for tank gas of 99.995 purity at one atmosphere, the required impurity pressure was about 3.5 microns, a pressure which the system would maintain indefinitely.

APPENDIX 5

FISSION FRAGMENT TRANSIT TIME

One surprising result of this study was the near constancy of the fission fragment transit time. The analysis of the decay curves was constrained by two conflicting requirements. The least square fit should start as early in time as possible since the nearer the peak, the greater the number of counts and, hence, the larger the statistical accuracy. However, if the fit was started too early, before the fission fragment had passed out of the field of view, the population would not be decaying with a simple exponential decay, and so the fit would be distorted.

In examining the early intensity curves, it was noted that the rise time was equal to about 4ns independent of gas pressure or molecular weight; a result which was thought to illustrate some limitation of the system. When the transit times were calculated using the expression in Chapter 3, it was found that in going from helium at six torr to argon at 800 torr, the transit time only changed from 4.28ns to 4.12ns. This result, while at first surprising, can be explained as follows: When the fission fragment first entered the gas, it was very highly charged and was traveling very fast; fast, that is, with respect to the orbital velocity of the electrons bound to the

target gas. If the velocity of the fission fragment compared to that of the bound electron is such that $v^2/u^2 >> 1$, where v is the velocity of the fission fragment and u is the vlocity of the bound electron, then the electron cloud around the atom or molecule does not have time to adjust to the rapidly passing microfield and inelastic collision occurs. The initial velocity of the fission fragment is 1.04×10^9cm/sec for the heavy fragment of 80 MeV and 1.37×10^9cm/sec for the light fragment of 106 MeV, which is to be compared with a typical orbital velocity of 4.4×10^{-8}cm/sec for the $1S^2$ state of helium

Thus, v^2/u^2 equals 5.6 for the heavy fragment and 9.7 for the light, both well above unity. When the fragment has slowed to the point where v^2/u^2 was equal to unity, the velocity of the fragment would still be 4.4×10^8cm/sec (about 10 MeV for the light and 30 MeV for the heavy fragment), but it would no longer undergo inelastic collisions with the electron cloud, and, hence cause no more excited states. At that velocity, the heavy fragment would have lost 50 MeV of its original 80 and the light, 95 MeV of its original 105 MeV. The significant result here was that even after the fission fragment had lost all the energy it could to the electrons, and so for the purpose of this experiment it could be said to have completed its transit, it was still traveling at no

mean speed, 4.4×10^8 cm/sec and crossed the chamber very rapidly. This then explains the near constancy of the intensity curve rise time and the calculated transit times:

1) Because the excitation cross-section is determined by velocity rather than energy (the Bethe-Born approximation).
2) Because the velocity goes as the square root of the energy.
3) Because even when the fission fragment has lost all the energy to the electrons that it can and is, therefore, no longer observable, it is still one speedy little mother. Thus, whatever happens to it in crossing the chamber affects the transit time hardly at all.

APPENDIX 6

^{252}Cf CHARACTERISTICS

The ^{252}Cf isotope used in this experiment was an open source made by evaporating an HCl solution of the metal onto a thin nickel disk. This isotope layer was only a few atoms thick and, thus, the energy spectrum of the emergent fission fragments was essentially the birth distribution and showed the familiar double humped shape (Fig. 14). The source had a nominal activity of 5μCi and weighed 0.01μg. The main characteristics of ^{252}Cf are shown in Table A.

Using these numbers, we may calculate the relevant characteristics of the actual source. These are shown in Table B. Measurements of the fission fragment and alpha rate, which were the only ones attempted, gave nearly identical numbers.

TABLE A

MAIN CHARACTERISTICS OF ^{252}Cf

Half-life:	2.646 y
Fission Fragment Energy:	Light, 105.71 MeV Heavy, 80.01 MeV
Fission Fragment Mass:	Light, 108.39 AMU Heavy, 143.61 AMU
Fission Activity:	16.8 μCi/μg
Fission Half-life:	85.5 y
Alpha Activity:	526 μCi/μg
Alpha Half-life:	2.731 y
Alpha to Fission Ratio:	31.3:1
Average Alpha Energy:	6.117 MeV (82%) 6.08 MeV (15%)
Neutrons Per Fission:	3.76
Neutron Activity:	63.2 μCi/μg
Neutron Emission Rate:	2.34×10^{12} $sec^{-1}g^{-1}$
Average Neutron Energy:	2.348 MeV
Gamma Energy:	43 keV
Beta Energy:	22 keV

TABLE B CHARACTERISTICS OF THE SOURCE	
Neutron Rate:	2.34×10^4 sec^{-1}
Gamma Rate:	1.3×10^5 sec^{-1}
Alpha Rate:	1.95×10^5 sec^{-1}
Fission Rate:	6200 sec^{-1}

BIBLIOGRAPHY

1. R. A. Walters, Excitation and Ionization of Gases by Fission Fragments, Ph.D. dissertation, University of Florida (1972).

2. R. N. Davie, Spectroscopy of Fission Fragment Excited Gases by Fission Fragments, Ph.D. dissertation, University of Florida (1975).

3. J. C. Guyot, Measurement of Atomic Metastable Densities in Noble Gas Plasmas Created by Nuclear Radiations, Ph.D. dissertation, University of Illinois at Urbana-Champaign (1971).

4. P. E. Theiss, Optical Emission and Kinetics of High-Pressure Radiation-Produced Noble Gas Plasmas, Ph.D. dissertation, University of Illinois at Urbana-Champaign (1971).

5. J. M. Calo, R. C. Axtmann, and R. G. Persing, Rev. Sci. Inst., 41, 11 (1970).

6. L. G. Christophorou, Atomic and Molecular Radiation Physics, Wiley Interscience, N.Y. (1971).

7. R. H. Lo and G. H. Miley, IEEE Trans. on Plasma Science (1974).

8. G. Herzberg, Molecular Spectra and Molecular Structure: I. Spectra of Diatomic Molecules, 2nd Ed., D. Van Nostrand, Princeton, N.J. (1950).

9. G. H. Miley and P. E. Theiss, Nuclear Applications, 6, (1969).

10. R. C. Axtmann and J. T. Sears, Nuc. Sci. & Eng., 23 (1965).

11. D. F. Keefer, Private Communication (1976).

12. W. K. MacGregor, Private Communication (1968).

13. M. E. Jones, Private Communication (1970).

14. R. A. Hefferlin, Private Communication (1975).

15. J. F. Davis, Kinetic and Experimental Study of Argon and Argon-Nitrogen Mixtures Excited by Fission Fragments, Ph.D. dissertation, University of Florida (1976).

16. R. Pagano and J. W. Wethington, Jr., Trans. Am. Nucl. Society, 14 (1971).

17. P. Pringsheim, Fluorescence and Phosphorescence, Interscience Publishers, N.Y. (1949).

18. F. Hiroyama and S. Lipskey, J. Chem. Phys., 51 (1969).

19. R. N. Davie, et al, Third Symposium on Uranium Plasmas, Princton, N.J. (1976).

20. E. T. Gerry, Appl. Phy. Lett., 1, 6 (1965).

21. R. A. Heustis, et al, Stanford Research Institute Technical Report 4, Project PYU-1925 (1975).

BIOGRAPHICAL SKETCH

George Robert Shipman was born January 3, 1944, in Bridgeport, Connecticut. He moved with his family to Orlando, Florida, in 1953. He attended Fletch Academy, Fletcher, North Carolina, and Forest Lake Academy, Maitland, Florida.

He received the Bachelor of Science degree at the University of Florida with a major in Physics in June, 1966, and was elected a member of Sigma Pi Sigma.

In 1968, he received the Master of Science degree in Astronomy with a minor in Physics from the University of Florida. He has held an Atomic Energy Commission traineeship and a departmental assistantship while in the Department of Nuclear Engineering Sciences.

I certify that I have read this study and that in my opinion it conforms to acceptable standards of scholarly presentation and is fully adequate, in scope and quality, as a dissertation for the degree of Doctor of Philosophy.

H. D. Campbell, Chairman
Associate Professor of Nuclear Engineering Sciences

I certify that I have read this study and that in my opinion it conforms to acceptable standards of scholarly presentation and is fully adequate, in scope and quality, as a dissertation for the degree of Doctor of Philosophy.

R. T. Schneider
Professor of Nuclear Engineering Sciences

I certify that I have read this study and that in my opinion it conforms to acceptable standards of scholarly presentation and is fully adequate, in scope and quality, as a dissertation for the degree of Doctor of Philosophy.

E. E. Carroll
Professor of Nuclear Engineering Sciences

I certify that I have read this study and that in my opinion it conforms to acceptable standards of scholarly presentation and is fully adequate, in scope and quality, as a dissertation for the degree of Doctor of Philosophy.

T. L. Bailey
Professor of Physics and Astronomy

I certify that I have read this study and that in my opinion it conforms to acceptable standards of scholarly presentation and is fully adequate, in scope and quality, as a dissertation for the degree of Doctor of Philosophy.

K. Y. Chen

K. Y. Chen
Associate Professor of Physics
and Astronomy

I certify that I have read this study and that in my opinion it conforms to acceptable standards of scholarly presentation and is fully adequate, in scope and quality, as a dissertation for the degree of Doctor of Philosophy.

G. R. Lebo

G. R. Lebo
Assistant Professor of Physics
and Astronomy

This dissertation was submitted to the Graduate Faculty of the College of Engineering and to the Graduate Council, and was accepted as partial fulfillment of the requirements for the Degree of Doctor of Philosophy.

December, 1976

Dean, College of Engineering

Dean, Graduate School